

Light color octet scalars in the minimal $SO(10)$ grand unification

Stefano Bertolini*

INFN, Sezione di Trieste, SISSA, via Bonomea 265, 34136 Trieste, Italy

Luca Di Luzio†

Institut für Theoretische Teilchenphysik, Karlsruhe Institute of Technology (KIT), D-76128 Karlsruhe, Germany

Michal Malinský‡

*Institute of Particle and Nuclear Physics, Faculty of Mathematics and Physics,
Charles University in Prague, V Holešovičkách 2, 180 00 Praha 8, Czech Republic*

We analyze the relation between the present (and foreseen) bounds on matter stability and the presence of TeV-scale color octet scalar states in nonsupersymmetric $SO(10)$ grand unification with one adjoint Higgs representation triggering the symmetry breaking. This scenario, discarded long ago due to tree-level tachyonic instabilities appearing in all phenomenologically viable breaking patterns, has been recently revived at the quantum level. By including the relevant two-loop corrections we find a tight correlation between the octet mass and the unification scale which either requires a light color octet scalar within the reach of the LHC or, alternatively, a proton lifetime accessible to the forthcoming megaton-scale facilities.

PACS numbers: 12.10.-g, 12.10.Kt, 14.80.-j

I. INTRODUCTION

The class of $SO(10)$ models where, the first step of the spontaneous symmetry breaking is driven by the vacuum expectation value (VEV) of a Higgs adjoint, was for a long time considered to be phenomenologically impracticable due to instabilities of the classical vacuum configurations supporting potentially viable symmetry breaking chains [1–4]. However, it was shown recently [5] that such instabilities can be removed at the quantum level and, thus, the nonsupersymmetric $SO(10)$ unification with the minimal Higgs content has been revived as a potentially realistic framework.

In a recent work [6] we analyzed a simple nonsupersymmetric $SO(10)$ gauge model with $45_H \oplus 126_H$ in the Higgs sector focusing on the details of the scalar spectrum as a key ingredient of a detailed understanding of the gauge unification constraints. Surprisingly, the theory turned out to be capable of supporting viable unifying patterns with the $B - L$ breaking scale stretching as high as 10^{14} GeV, right within the ballpark assumed for a natural implementation of the seesaw for neutrinos (see [7] for a systematic discussion).

In particular, we pointed out that a seesaw scale in the $10^{13} - 10^{14}$ GeV range is obtained along the breaking chains featuring intermediate $SU(3)_c \otimes SU(2)_L \otimes SU(2)_R \otimes U(1)_{B-L}$ or $SU(4)_C \otimes SU(2)_L \otimes U(1)_R$ gauge symmetries when either an intermediate-scale color sextet (transforming as a weak triplet) or a light color octet

(weak doublet) appear in the scalar spectrum; the latter case is especially interesting because there the unification constraints allow for a colored scalar octet in the vicinity of the electroweak scale which can be very interesting from the collider physics point of view. On top of that, the mass of the octet turns out to be anticorrelated with the masses of the grand unified theory (GUT) scale vector bosons governing the $d = 6$ proton decay and, hence, a lower bound on the matter lifetime translates to an upper bound on the octet mass.

From the bottom-up perspective, the existence of light color octet (or sextet) scalars in the sub-TeV domain was recently advocated in [8, 9] as a possible explanation for the $H \rightarrow \gamma\gamma$ excess observed in the LHC data [10–12]. To this end, it has been pointed out [13] that only the standard Higgs doublets or color octets with the Higgs-like weak quantum numbers can naturally couple to quarks without introducing large flavor changing neutral currents (FCNC). The implementation of a custodial symmetry in these settings can then help further with taming the associated radiative corrections so that a standard-model-like (SM-like) setup is maintained. Light colored scalars have been widely discussed in connection to various new physics scenarios and in the recent years with great emphasis on their implications for the LHC physics [14–49].

In this paper we restrict the systematic discussion of ref. [6] to the possibility of a light color octet scalar. We refine the analysis of gauge unification to the two-loop level and we enter the details of the calculation of the width of the dominant proton decay mode. We entirely focus on the minimal $SO(10)$ light color octet (weak doublet) scenario since, unlike the intermediate-scale sextet case (with the typical sextet mass at about 10^{11} GeV), it is far more interesting from the collider perspective.

* bertolin@sissa.it

† diluzio@kit.edu

‡ malinsky@ipnp.troja.mff.cuni.cz

We find that the two-loop corrections strengthen the correlation between the scalar octet mass and the unification scale in such a way that strict bounds on the scalar mass can be derived from the proton lifetime limits. In particular, for the present day proton stability constraints we find a conservative 2000 TeV upper bound on the color octet mass which is further pushed down to about 20 TeV in case of a null result in the next generation proton decay searches. In any case, a large fraction of the parameter space of the minimal $SO(10)$ GUT allows for a scalar octet mass in the TeV (and even sub-TeV) regime.

II. LIGHT COLOR OCTET SCALAR IN THE MINIMAL $SO(10)$

A. The 45-126 Higgs model

We consider an $SO(10)$ Higgs sector including one 45_H adjoint representation together with one 126_H ¹. The consideration of an additional 10_H (or two) is not relevant for the purpose of this paper and we shall comment on it only later in Sect. II C 4 b.

The most general renormalizable scalar potential that can be written with just 45_H and 126_H at hand reads

$$V = V_{45} + V_{126} + V_{\text{mix}}, \quad (1)$$

where

$$V_{45} = -\frac{\mu^2}{2}(\phi\phi)_0 + \frac{a_0}{4}(\phi\phi)_0(\phi\phi)_0 + \frac{a_2}{4}(\phi\phi)_2(\phi\phi)_2, \quad (2)$$

$$\begin{aligned} V_{126} = & -\frac{\nu^2}{5!}(\Sigma\Sigma^*)_0 \\ & + \frac{\lambda_0}{(5!)^2}(\Sigma\Sigma^*)_0(\Sigma\Sigma^*)_0 + \frac{\lambda_2}{(4!)^2}(\Sigma\Sigma^*)_2(\Sigma\Sigma^*)_2 \\ & + \frac{\lambda_4}{(3!)^2(2!)^2}(\Sigma\Sigma^*)_4(\Sigma\Sigma^*)_4 + \frac{\lambda'_4}{(3!)^2}(\Sigma\Sigma^*)_{4'}(\Sigma\Sigma^*)_{4'} \\ & + \frac{\eta_2}{(4!)^2}(\Sigma\Sigma)_2(\Sigma\Sigma)_2 + \frac{\eta_2^*}{(4!)^2}(\Sigma^*\Sigma^*)_2(\Sigma^*\Sigma^*)_2, \end{aligned} \quad (3)$$

$$\begin{aligned} V_{\text{mix}} = & \frac{i\tau}{4!}(\phi)_2(\Sigma\Sigma^*)_2 + \frac{\alpha}{2 \cdot 5!}(\phi\phi)_0(\Sigma\Sigma^*)_0 \\ & + \frac{\beta_4}{4 \cdot 3!}(\phi\phi)_4(\Sigma\Sigma^*)_4 + \frac{\beta'_4}{3!}(\phi\phi)_{4'}(\Sigma\Sigma^*)_{4'} \\ & + \frac{\gamma_2}{4!}(\phi\phi)_2(\Sigma\Sigma)_2 + \frac{\gamma_2^*}{4!}(\phi\phi)_2(\Sigma^*\Sigma^*)_2. \end{aligned} \quad (4)$$

¹ Minimally, one would prefer to consider 16_H in place of 126_H . On the other hand $\langle 16_H \rangle$ breaks the $B-L$ symmetry only by one unit and, thus, the seesaw requires a pair of $\langle 16_H \rangle$ insertions. This can be implemented at the renormalizable level by, e.g., a variant of the Witten's radiative mechanism [50–52] or, giving up renormalizability, by a $d=5$ operator. In either case the “effective” $\Delta(B-L)=2$ seesaw scale is further suppressed with respect to the “genuine” $B-L$ breaking VEV and the light neutrino masses are typically overshoot by many orders of magnitude.

Here the ϕ and Σ stand for the components of 45_H and 126_H , respectively. The detailed breakdown of all the contractions (with the subscripts denoting the number of open indices in the relevant brackets) is given in Appendix A of ref. [6]. All couplings are real but η_2 and γ_2 .

There are, in general, three SM singlets in the reducible $45_H \oplus 126_H$ representation of $SO(10)$. Using $BL \equiv (B-L)$ and labeling the field components with respect to the $3_c 2_L 2_R 1_{BL}$ (i.e., $SU(3)_c \otimes SU(2)_L \otimes SU(2)_R \otimes U(1)_{BL}$) algebra, the SM singlets reside in the $(1, 1, 1, 0)$ and $(1, 1, 3, 0)$ submultiplets of 45_H and in the $(1, 1, 3, +2)$ component of 126_H . In what follows we shall denote

$$\langle (1, 1, 1, 0) \rangle \equiv \omega_{BL}, \quad \langle (1, 1, 3, 0) \rangle \equiv \omega_R, \quad \langle (1, 1, 3, +2) \rangle \equiv \sigma, \quad (5)$$

where $\omega_{BL,R}$ are real and σ can be made real by a phase redefinition of the 126_H . Different VEV configurations trigger the spontaneous breakdown of the $SO(10)$ symmetry into several qualitatively distinct subgroups. Namely, for $\sigma = 0$ one finds (in an obvious notation)

$$\begin{aligned} \omega_R = 0, \omega_{BL} \neq 0 : & \quad 3_c 2_L 2_R 1_{BL}, \\ \omega_R \neq 0, \omega_{BL} = 0 : & \quad 4_C 2_L 1_R, \\ \omega_R \neq 0, \omega_{BL} \neq 0 : & \quad 3_c 2_L 1_R 1_{BL}, \\ \omega_R = -\omega_{BL} \neq 0 : & \quad \text{flipped } 5' 1_{Z'}, \\ \omega_R = \omega_{BL} \neq 0 : & \quad \text{standard } 5 1_Z, \end{aligned} \quad (6)$$

with $5 1_Z$ and $5' 1_{Z'}$ standing for the two inequivalent embeddings of the SM hypercharge operator Y into $SU(5) \otimes U(1) \subset SO(10)$ usually called the “standard” and the “flipped” $SU(5)$ scenarios [53, 54], respectively. In the standard case, $Y = T_R^3 + \frac{1}{2}T_{BL}$ belongs to the $SU(5)$ algebra and the orthogonal Cartan generator Z is given by $Z = -4T_R^3 + 3T_{BL}$. In the flipped ($5' 1_{Z'}$) case, the right-handed isospin assignment of quarks and leptons is turned over so that the flipped hypercharge generator reads $Y' = -T_R^3 + \frac{1}{2}T_{BL}$. Accordingly, the additional $U(1)_{Z'}$ generator reads $Z' = 4T_R^3 + 3T_{BL}$ (for further details see, e.g., ref. [5]).

For $\sigma \neq 0$ all the intermediate gauge symmetries (6) are spontaneously broken down to the SM group, with the exception of the last case which maintains the $SU(5)$ subgroup unbroken.

B. Gauge unification and the scalar octet mass

There are several basic criteria we impose on each vacuum of the theory featuring a light color octet scalar. Besides the very consistency of the gauge unification picture at two loops we demand compatibility with the proton lifetime constraints and require a reasonably high seesaw scale in order to support a renormalizable (and, hence, potentially predictive) implementation of the seesaw mechanism. This program for the minimal $SO(10)$ setting here considered has been initiated in [6]. The goal of the current study is to include the relevant two-loop running effects and to assess their impact on the breaking pattern and the scalar spectrum.

1. Two-loop gauge unification constraints

The Higgs setting we are considering here (i.e., with an adjoint Higgs driving the $SO(10)$ breaking) was shown to provide phenomenologically interesting breaking patterns only if at least the one-loop effective potential is considered [5]. Gauge unification constraints and the shape of the scalar spectrum have been discussed in [6], where it is shown that an acceptable $B - L$ scale for the renormalizable seesaw implementation is obtained only if the scalar spectrum exhibits "light" colored scalar states (in particular, an octet or a sextet). This result improved on previous analyses (see for instance [7] and refs. [55–57] for earlier studies) based on the minimal survival hypothesis (MSH) [58, 59], where just the scalar spectrum necessary for the spontaneous symmetry breaking at each stage is assumed at the corresponding scale. This allows a for systematic analysis, albeit preliminary to a detailed study of the vacuum constraints.

In what follows we shall consider only the setting with the light color octet scalar transforming as a weak doublet, i.e., $H_8 \equiv (8, 2, +\frac{1}{2})$, for its potential relevance to the TeV physics scale. A discussion of the shape of the relevant one-loop scalar spectrum, the effects of the heavy scalar thresholds and the constraints obtained from the gauge unification and the absolute neutrino mass scale will be given in Section II C.

a. The tree-level scalar spectrum. Adopting the convention in which the mass term in the Lagrangian is written as $\frac{1}{2}\psi^T M^2 \psi$, where $\psi = (\phi, \Sigma^*, \Sigma)$ is a 297-dimensional vector, the scalar spectrum is obtained readily by evaluating the relevant functional scalar mass matrix of the schematic form

$$M^2(\phi, \Sigma^*, \Sigma) = \begin{pmatrix} V_{\phi\phi} & V_{\phi\Sigma^*} & V_{\phi\Sigma} \\ V_{\Sigma^*\phi} & V_{\Sigma^*\Sigma^*} & V_{\Sigma^*\Sigma} \\ V_{\Sigma\phi} & V_{\Sigma\Sigma^*} & V_{\Sigma\Sigma} \end{pmatrix} \quad (7)$$

on the SM vacuum. The subscripts here denote the derivatives of the scalar potential with respect to a specific set of fields. Subsequently, this matrix can be brought to a block-diagonal form (i.e., into the SM basis) by a unitary transformation. The complete tree-level spectrum is found in Appendix B of ref. [6].

b. One-loop scalar spectrum. Conceptually, a complete two-loop analysis of the unification pattern requires a thorough understanding of the one-loop spectrum of the theory. This, however, is extremely demanding in full generality. On the other hand, for the sake of the current analysis it is sufficient to focus on the most prominent one-loop corrections to the scalar masses, namely, those that cure the instabilities of the tree level potential [5].

The leading loop-induced nonlogarithmic correction in the scalar sector comes from tadpoles [60] which, among other contributions, yield the "universal" ($SO(10)$ symmetric) shift to the scalar masses via the τ term in the potential. It is not difficult to see that the only source of a τ^2 -proportional nonlogarithmic term is associated to the renormalization of the stationarity conditions imposed on

the scalar potential. Diagrammatically, it corresponds to a special cluster of one-loop graphs contributing to the one-point function of 45_H , cf. [6]. Given the $SO(10)$ structure of the relevant τ -vertex in (4) one finds

$$\Delta M_{\tau^2}^2 = \frac{35\tau^2}{32\pi^2} \quad (8)$$

that can be viewed as a typical one-loop correction of the scalar masses in the vicinity of the GUT scale. This is numerically relevant namely for those states in 45_H that are tachyonic at the tree-level [6], thus allowing for a simplified treatment of the scalar spectrum.

c. Effective gauge theories and matching scales: The generic structure of the vacua supporting a light color octet scalar, namely $\omega_R \gg (\omega_{BL}, \sigma)$, was discussed in [6]. This suggests that the breaking of the $SO(10)$ gauge symmetry can be conveniently described by the following series of effective gauge theories [61]

$$\begin{array}{c} SO(10) \\ \downarrow^{\mu_2} \\ SU(4)_C \otimes SU(2)_L \otimes U(1)_R \\ \downarrow^{\mu_1} \\ SU(3)_c \otimes SU(2)_L \otimes U(1)_Y \quad (\text{SM} + H_8) \\ \downarrow^{\mu_0} \\ SU(3)_c \otimes SU(2)_L \otimes U(1)_Y \quad (\text{SM}) \end{array} \quad (9)$$

where $\mu_2 > \mu_1 > \mu_0$ denote the relevant matching scales. Unlike for the first two steps where the gauge symmetry of the effective theory changes (as does the associated vector boson spectrum with all subtleties associated to that), the third arrow corresponds to the decoupling of just the light H_8 at a certain scale μ_0 with no change in the gauge sector and, as such, it is almost trivial. In the numerical simulation in Sect. II C the scales $\mu_{1,2}$ are naturally chosen in the vicinity of the masses of the gauge bosons associated to the two relevant symmetry breakings triggered by the VEVs ω_R and σ , i.e.,

$$\mu_2 = g_G^0 \omega_R, \quad \mu_1 = g_G^0 \sigma, \quad (10)$$

where $g_G^0 = 0.6$ is the typical value of the gauge couplings at (or around) the GUT scale identified in [6].

Strictly speaking, the scheme (9) is naturally implied for $\sigma \gtrsim \omega_{BL}$ which, indeed, corresponds to our main interest in settings with a maximum allowed σ , cf. Section II B 3. In the opposite case, i.e., for $\omega_{BL} \gtrsim \sigma$, one may for simplicity consider an extra stage with an intermediate $SU(3)_c \otimes SU(2)_L \otimes U(1)_R \otimes U(1)_{BL}$ symmetry. Since, however, this is mostly a matter of language (as the difference between the two approaches can be essentially subsumed into a set of extra threshold effects in the simple scheme above) we shall consider only four effective theories along with three effective matching scales for all settings. The interested reader can find further remarks on the consistency of this approach in section II C 1.

d. The two-loop beta functions: In what follows we shall pass through all the steps in (9) and list all the a_i

and b_{ij} coefficients entering the two-loop renormalization group equations for the gauge couplings [62–65]²

$$\frac{d}{dt}\alpha_i^{-1} = -a_i - \frac{b_{ij}}{4\pi}\alpha_j, \quad (11)$$

where

$$t = \frac{1}{2\pi} \log \mu/M_Z \quad (12)$$

provided

$$a_i = -\frac{11}{3}C_2(G_i) + \frac{4}{3}\kappa S_2(F_i) + \frac{1}{3}\eta S_2(S_i), \quad (13)$$

$$b_{ij} = \left[-\frac{34}{3}(C_2(G_i))^2 + \left(4C_2(F_i) + \frac{20}{3}C_2(G_i) \right) \kappa S_2(F_i) + \left(4C_2(S_i) + \frac{2}{3}C_2(G_i) \right) \eta S_2(S_i) \right] \delta_{ij} + 4 \left[\kappa C_2(F_j) S_2(F_i) + \eta C_2(S_j) S_2(S_i) \right] \quad (14)$$

(no summation over i). Here S_2 and C_2 denote the index (including multiplicity factors) and the quadratic Casimir of a given representation, $\kappa = 1, \frac{1}{2}$ for Dirac and Weyl fermions and $\eta = 1, \frac{1}{2}$ for complex and real scalar fields, respectively. For a detailed account of the subtleties related to the case with more than a single abelian gauge factor the interested reader may refer to the discussion in ref. [7] and references therein. For $|\omega_j(t-t_0)| < 1$, with $\omega_j \equiv a_j \alpha_j(t_0)$, the expression

$$\alpha_i^{-1}(t) - \alpha_i^{-1}(t_0) = -a_i(t-t_0) + \frac{b_{ij}}{4\pi a_j} \log[1 - \omega_j(t-t_0)] \quad (15)$$

is, to a great accuracy, a solution of Eq. (11).

Above μ_2 the spectrum of the theory under consideration is defined by the 45-dimensional adjoint representation containing the gauge fields, three copies of the 16-dimensional matter spinors, a real 45-dimensional adjoint scalar and a complex 126-dimensional antiselfdual component of the 5-index antisymmetric $SO(10)$ tensor. This altogether yields

$$a = -37/3, \quad b = 9529/6. \quad (16)$$

The scale μ_2 characterizes the $SO(10)$ breaking to $SU(4)_C \otimes SU(2)_L \otimes U(1)_R$. At this stage, the propagating gauge bosons fill the $(15, 1, 0) \oplus (1, 3, 0) \oplus (1, 1, 0)$ reducible representation of the gauge group, together

with matter multiplets in three copies of the $(4, 2, 0) \oplus (\bar{4}, 1, +\frac{1}{2}) \oplus (\bar{4}, 1, -\frac{1}{2})$ representation and complex scalars in $(\bar{10}, 1, -1) \oplus (15, 2, +\frac{1}{2})$. Note that the latter is just the minimal set of fields that may trigger the subsequent steps of the gauge symmetry breaking and, thus, the natural expectation of the minimal survival shape of the scalar spectrum is conformed. With all this at hand one has

$$a_i = (-7, -\frac{5}{6}, \frac{59}{6}), \quad b_{ij} = \begin{pmatrix} \frac{265}{2} & \frac{57}{2} & \frac{43}{2} \\ \frac{285}{2} & \frac{217}{6} & \frac{15}{2} \\ \frac{645}{2} & \frac{45}{2} & \frac{101}{2} \end{pmatrix}, \quad (17)$$

where $i, j \in \{4_C, 2_L, 1_R\}$.

Below μ_1 the effective theory is the SM plus H_8 scalar. The gauge fields are grouped into $(8, 1, 0) \oplus (1, 3, 0) \oplus (1, 1, 0)$ while the matter resides in three copies of $(3, 2, \frac{1}{6}) \oplus (1, 2, -\frac{1}{2}) \oplus (\bar{3}, 1, -\frac{2}{3}) \oplus (\bar{3}, 1, +\frac{1}{3}) \oplus (1, 1, -1)$. The surviving H_8 scalars transform as $(8, 2, +\frac{1}{2}) \oplus (1, 2, +\frac{1}{2})$. The RGE beta coefficients read:

$$a_i = (-5, -\frac{11}{6}, \frac{49}{10}), \quad b_{ij} = \begin{pmatrix} 58 & \frac{45}{2} & \frac{47}{10} \\ 60 & \frac{139}{6} & \frac{33}{10} \\ \frac{188}{5} & \frac{99}{10} & \frac{271}{50} \end{pmatrix}, \quad (18)$$

where $i, j \in \{3_c, 2_L, 1_Y\}$.

After H_8 is integrated out (at $\mu_0 \equiv M_8$), the minimal set of the SM fields (including one Higgs doublet) yields:

$$a_i = (-7, -\frac{19}{6}, \frac{41}{10}), \quad b_{ij} = \begin{pmatrix} -26 & \frac{9}{2} & \frac{11}{10} \\ 12 & \frac{35}{6} & \frac{9}{10} \\ \frac{44}{5} & \frac{27}{10} & \frac{199}{50} \end{pmatrix}. \quad (19)$$

At M_Z (i.e., at $t = 0$) the $SU(5)$ -normalized SM gauge couplings are required to fall into the current 1- σ bands

$$\begin{aligned} \alpha_1 &= 0.0169225 \pm 0.0000039, \\ \alpha_2 &= 0.033735 \pm 0.000020, \\ \alpha_3 &= 0.1173 \pm 0.0007, \end{aligned} \quad (20)$$

where these data refer to the modified minimal subtraction scheme ($\overline{\text{MS}}$) in the full SM, i.e. the top being not integrated out [66–68].

e. Threshold corrections. What remains to be detailed is the matching between all the gauge theories in (9). The general form of the one-loop matching condition between effective theories in the framework of dimensional regularization has been discussed in [61, 69]. Let us consider first a simple gauge group G spontaneously broken into subgroups G_i . The one-loop matching for the gauge couplings can be then written as

$$g_i^{-2} = g^{-2} - \lambda_i(\mu), \quad (21)$$

where

$$\begin{aligned} \lambda_i(\mu) &= \frac{1}{48\pi^2} \left[\text{Tr } T_{iV}^2 - 21 \text{Tr } T_{iV}^2 \log \frac{M_V}{\mu} \right. \\ &\quad \left. + 8 \text{Tr } T_{iF}^2 \log \frac{M_F}{\mu} + \text{Tr } T_{iS}^2 \log \frac{M_S}{\mu} \right] \end{aligned} \quad (22)$$

² The two-loop contribution of the Yukawa couplings is here neglected. As a matter of fact we checked that the top-Yukawa coupling contributes to less than the 10% to the difference between the one- and two-loop results. In addition, such a contribution produces an almost uniform shift on the evolved gauge couplings, thus affecting only the determination of the unified gauge coupling (cf. e.g. the discussion in Sect. IV D of [7]).

with V , F and S denoting the massive vectors, fermions and scalars that are integrated out at the matching scale μ (classified with respect to the preserved symmetries G_i)³. Let us also note that T_i stand for the corresponding group generators and the relevant multiplicities are looked after the traces.

In the notation of Eq. (14) the matching corrections can be written as

$$\lambda_i(\mu) = \frac{1}{48\pi^2} S_2(V_i) + \frac{1}{8\pi^2} \left[-\frac{11}{3} \text{Tr} T_{V_i}^2 \log \frac{M_{V_i}}{\mu} \right. \\ \left. + \frac{4}{3} \kappa \text{Tr} T_{F_i}^2 \log \frac{M_{F_i}}{\mu} + \frac{1}{3} \eta \text{Tr} T_{S_i}^2 \log \frac{M_{S_i}}{\mu} \right], \quad (23)$$

where the (Feynman gauge) Goldstone bosons have been conveniently included in the scalar part of the expression. Note that $S_2(V_i)$ can here be written as $C_2(G) - C_2(G_i)$.

When multiple $U(1)$ factors are present one must be careful about the abelian mixing effects; in what follows we shall follow the notation and discussion of ref. [7]. Consider the breaking of N copies of $U(1)$ gauge factors to a subset of M elements $U(1)$ (with $M < N$). Denoting by T_n ($n = 1, \dots, N$) and by \tilde{T}_m ($m = 1, \dots, M$) their properly normalized generators we have

$$\tilde{T}_m = P_{mn} T_n \quad (24)$$

with the orthogonality condition $P_{mn} P_{m'n} = \delta_{mm'}$. Let us denote by g_{na} ($n, a = 1, \dots, N$) and by \tilde{g}_{mb} ($m, b = 1, \dots, M$) the matrices of abelian gauge couplings above and below the breaking scale respectively. Writing the abelian gauge boson mass matrix in the broken vacuum and identifying the massless states one finds the following matching condition

$$(\tilde{g}g^T)^{-1} = P (gg^T)^{-1}_{\text{eff}} P^T, \quad (25)$$

where

$$g_{\text{eff AB}}^{-2} \equiv g_{AB}^{-2} - \lambda_{AB}(\mu), \quad (26)$$

with $A, B = 1, \dots, N$. Equation (25) depends on the choice of basis for the $U(1)$ charges (via P) but it is invariant under orthogonal rotations of the gauge boson fields ($gO^T O g^T = gg^T$). Notice that whenever the decoupled states are classified by multiple $U(1)$ charges the presence of nonvanishing off-diagonal entries in λ_{AB} is crucial for the correct matching even if no multiple- $U(1)$ -symmetric stage is actually considered (i.e., for diagonal g_{AB}^{-2}).

The general case of a gauge group $U(1)_1 \otimes \dots \otimes U(1)_N \otimes G_1 \otimes \dots \otimes G_{N'}$ spontaneously broken to $U(1)_1 \otimes \dots \otimes U(1)_M$ with $M \leq N + N'$ is taken care of by replacing $(gg^T)^{-1}$ in Eq. (25) with the block-diagonal $(N + N') \times (N + N')$ matrix

$$(GG^T)^{-1} = \text{Diag} [(gg^T)^{-1}, g_i^{-2}], \quad (27)$$

³ As a matter of fact, one may choose any proper subgroup G'_i of G_i for the classification of the decoupled fields. This freedom is ensured by the identity $S_2(R^G) = \sum_{R \in G'} S_2(R^{G'})$.

thus providing, together with the extended version of Eq. (24), the necessary generalization of Eq. (21).

At the $SO(10) \rightarrow SU(4)_C \otimes SU(2)_L \otimes U(1)_R$ breaking scale μ_2 the following components are decoupled (the subscripts denote the origin of the listed multiplets in terms of the $SO(10)$ scalar irreps [cf. also TABLES IV and V], while the superscripts V and GB indicate their vector and/or Goldstone-boson nature): $(1, 1, \pm 1)^V$, $(1, 1, \pm 1)_{45}^{\text{GB}}$, $(6, 2, \pm \frac{1}{2})^V$, $(6, 2, \pm \frac{1}{2})_{45}^{\text{GB}}$, $(6, 1, 0)_{126}$, $(10, 3, 0)_{126} + \text{h.c.}$, $(\overline{10}, 1, 0)_{126} + \text{h.c.}$, $(\overline{10}, 1, +1)_{126} + \text{h.c.}$, $(1, 1, 0)_{45}$, $(1, 3, 0)_{45}$, $(15, 1, 0)_{45}$, and the heavy eigenstate of the $(15, 2, \pm \frac{1}{2})_{126} + \text{h.c.}$ system. Let us stress that the last item of the list above corresponds to the state orthogonal to the component hosting the light SM doublet Higgs that has been identified as “active” throughout the 421 stage in Sect. IIB 1 d.

At the $SU(4)_C \otimes SU(2)_L \otimes U(1)_R \rightarrow \text{SM} + H_8$ matching scale, we have to take into account that the SM hypercharge generator is a weighted average of that of the $U(1)_{BL}$ subgroup of $SU(4)_C$ and the $U(1)_R$ charge. In terms of the canonically normalized abelian charges one has $Y = \sqrt{\frac{3}{5}} T_R^3 + \sqrt{\frac{2}{5}} X$, where $X = \sqrt{\frac{3}{8}} (B - L)$ obeys $\text{Tr} X^2 = 1$ in the defining 10-dimensional vector representation of $SO(10)$. In what follows, it will be useful to define the hypercharge projector $P_Y = \left(\sqrt{\frac{3}{5}}, \sqrt{\frac{2}{5}} \right)$ for which $Y = P_Y (T_R^3, X)^T$.

In terms of the $3_{c2L1R1BL}$ quantum numbers, the fields that decouple at μ_1 are (with subscripts and superscripts as above): $(\overline{3}, 1, 0, -\frac{4}{3})^V + \text{h.c.}$, the light eigenstate of the $(\overline{3}, 1, -1, +\frac{2}{3})_{126} \oplus (\overline{3}, 1, 0, -\frac{4}{3})_{45} + \text{h.c.}$ system playing the role of the associated Goldstone boson⁴, $(1, 1, -1, +2)_{126} + \text{h.c.}$, $(\overline{6}, 1, -1, -\frac{2}{3})_{126}$, $(3, 2, +\frac{1}{2}, +\frac{4}{3})_{126} + \text{h.c.}$ and $(3, 2, -\frac{1}{2}, +\frac{4}{3})_{126} + \text{h.c.}$. An explicit example of the one-loop massive spectrum can be found in TABLE II. With all this at hand one can construct the corresponding 2×2 abelian matching matrix,

$$\lambda(\mu_1) = \begin{pmatrix} \lambda_{RR} & \lambda_{RX} \\ \lambda_{XR} & \lambda_{XX} \end{pmatrix}, \quad (28)$$

which subsequently enters the hypercharge matching condition

$$\alpha_Y^{-1}(\mu_1) = 4\pi P_Y [(GG^T)^{-1}(\mu_1) - \lambda(\mu_1)] P_Y^T. \quad (29)$$

In particular,

$$4\pi (GG^T)^{-1}(\mu_1) = \begin{pmatrix} \alpha_R^{-1}(\mu_1) & 0 \\ 0 & \alpha_4^{-1}(\mu_1) \end{pmatrix} \quad (30)$$

⁴ Even though the specific shape of the λ matrix (28) does depend on the details of the projection of the light eigenstate onto the two underlying components $(\overline{3}, 1, -1, +\frac{2}{3})_{126} \oplus (\overline{3}, 1, 0, -\frac{4}{3})_{45}$ there is actually no need to worry about this because both these components individually provide the same contribution to the $P_Y \lambda(\mu_1) P_Y^T$ factor in (29) and so does any of their properly normalised linear combinations.

is the matrix of the abelian gauge couplings which, in the case of our interest, is trivially diagonal since there is no explicit intermediate 3211 running in the relevant sequence of the effective gauge theories (9). A specific example of the $\lambda(\mu_1)$ matrix is reported in Appendix B.

Finally, at μ_0 fixed to the mass of H_8 (henceforth denoted by M_8) the effective theory becomes the pure SM. Needless to say, since the matching scale is conveniently chosen at the mass of the decoupled state, the matching is technically trivial.

2. Proton lifetime limits

a. Gauge-induced $d = 6$ proton decay: With a detailed information on the heavy spectrum of the model at hand one can rather accurately estimate the proton lifetime for all specific settings of interest. The master formula adjusted for the $SO(10)$ gauge content reads [33, 70]

$$\Gamma(p \rightarrow \pi^0 e^+) = \frac{\pi}{4} A_L^2 (1 + F + D)^2 \frac{|\alpha|^2}{f_\pi^2} m_p \alpha_G^2 \times \left[A_{SR}^2 \left(\frac{1}{M_{(X,Y)}^2} + \frac{1}{M_{(X',Y')}^2} \right)^2 + \frac{4A_{SL}^2}{M_{(X,Y)}^4} \right], \quad (31)$$

where $A_L = 1.25$ is the factor encoding the renormalization from the electroweak scale to the proton mass, $D = 0.81$, $F = 0.44$, $\alpha = -0.011 \text{ GeV}^3$ and $f_\pi = 139 \text{ MeV}$ are phenomenological parameters given by the chiral perturbation theory and lattice, $m_p = 938.3 \text{ MeV}$ is the proton mass and α_G is the GUT-scale gauge coupling. Let us also note that A_{SL} and A_{SR} are the renormalization factors of the relevant $d = 6$ proton decay operators from the GUT scale to the weak scale,

$$A_{SL(R)} = \prod_{i=1}^3 \prod_{P}^{M_Z \leq m_P < M_G} \left[\frac{\alpha_i(m_{P+1})}{\alpha_i(m_P)} \right]^{\frac{\gamma_{L(R)i}}{\sum_Q^{M_Z \leq m_Q \leq m_P} \Delta a_{iQ}}}. \quad (32)$$

Here, $\gamma_L = (\frac{23}{20}, \frac{9}{4}, 2)$, $\gamma_R = (\frac{11}{20}, \frac{9}{4}, 2)$, P and Q are labels of states relevant at each stage and Δa_{iQ} is the contribution of the field Q to the one-loop beta function; cf. Sect. II B 1 d. Furthermore, $M_{(X,Y)}$ and $M_{(X',Y')}$ denote the masses of the underlying GUT-scale gauge bosons (i.e., those transforming, respectively, as $(\bar{3}, 2, +\frac{5}{6})$ and $(\bar{3}, 2, -\frac{1}{6})$ under the SM gauge group). The latter are given, for the model under consideration, in Appendix C of ref. [6].

Due to the lack of information about the flavor sector of the theory, we have set all the flavor matrices governing the baryon and lepton number violating currents [71, 72] coupled to the heavy gauge fields to a 3×3 unit matrix; hence, we do not entertain any accidental cancellations in the relevant amplitudes which, in turn, makes our results conservative.

Given this, we shall implement namely the basic constraint corresponding to the current best Super-

Kamiokande (SK) limit [73]:

$$\tau(p \rightarrow e^+ \pi^0)_{\text{SK}, 2012} > 1.3 \times 10^{34} \text{ years}, \quad (33)$$

together with a pair of speculative Hyper-Kamiokande (HK) limits that are assumed to be reached by 2025 and 2040, respectively [74]:

$$\tau(p \rightarrow e^+ \pi^0)_{\text{HK}, 2025} > 9 \times 10^{34} \text{ years}, \quad (34)$$

$$\tau(p \rightarrow e^+ \pi^0)_{\text{HK}, 2040} > 2 \times 10^{35} \text{ years}. \quad (35)$$

In all figures of the next section, points obeying these three limits shall be, consecutively, denoted by light grey, dark grey and black colors.

b. Scalar-induced $d = 6$ proton decay: In general, the scalar-induced $d = 6$ proton decay operators are expected to be suppressed with respect to the gauge-driven ones due to the extra flavor factors associated to the first generation Yukawa couplings in the relevant baryon-number-violating currents. In the framework under consideration this expectation is further justified by the fact that the potentially dangerous colored triplets (Δ_c) never fall far from the GUT scale and, thus, never really compete with the gauge sector. To be on the safe side, we shall follow the strategy defined in the previous one-loop analysis [6] and implement a conservative lower bound of $m_{\Delta_c} \gtrsim 10^{14} \text{ GeV}$.

c. $d > 6$ induced proton decay: Due to the rather specific shape of the scalar spectrum and, in particular, the absence of baryon number violation in the H_8 couplings, the $d > 6$ proton decay is expected to be highly suppressed with respect to the $d = 6$ type of transitions. For further comments, the interested reader is deferred to Sect. III of reference [6].

3. Absolute neutrino mass scale

Another phenomenological issue we shall consider concerns the seesaw mechanism, which, for a potentially predictive scheme, is implemented at the renormalizable level via the VEVs of the relevant RH and LH triplets from 126_H . Assuming that the associated Yukawa coupling of 126_H is of order 1, the natural size of the seesaw scale (i.e., the VEV of the RH triplet) is in the 10^{13} GeV ballpark (and larger for smaller 126_H Yukawa couplings). Thus, in what follows, we show our results for two conservative regions corresponding to $\sigma \gtrsim 10^{12} \text{ GeV}$ and $\sigma \gtrsim 10^{13} \text{ GeV}$, respectively. On the other hand, as we shall see, these limits do not affect the absolute upper bound for M_8 in any substantial manner, cf. Fig. 3.

C. Results

The discussion of the results of the numerical simulation shall be divided into two parts. First, we shall discuss the shape of the parameter space that remains open

when the two-loop gauge unification and the proton lifetime constraints in Eqs. (33)–(35) are taken into account. Secondly, we shall discuss the general upper bounds on M_8 and their possible changes when, e.g., additional requirements related to the absolute neutrino mass scale in renormalizable implementations of the seesaw are imposed, cf. Sect. IIB 3. Finally, we shall briefly comment on the robustness of the results with respect to the variation of the intermediate matching scales, the possible effects of an additional 10_H in the Higgs sector and other relevant sources of uncertainties.

1. Consistent two-loop gauge unification

The shape of the relevant part of the parameter space corresponding to a stable vacuum supporting consistent gauge unification patterns with a light H_8 , compatible with the current proton lifetime limits, is best seen from the $\omega_{BL} - \sigma$ plane depicted in Fig. 1. The two regimes associated to the points above and below the $\omega_{BL} = \sigma$ diagonal correspond to the “shortened” $SO(10) \rightarrow 4_C 2_L 1_R \rightarrow \text{SM} + H_8 \rightarrow \text{SM}$ symmetry-breaking chain (upper-left part of Fig. 1) and to the “sliding σ regime” underpinning the $SO(10) \rightarrow 4_C 2_L 1_R \rightarrow 3_c 2_L 1_R 1_{BL} \rightarrow \text{SM} + H_8 \rightarrow \text{SM}$ symmetry-breaking pattern (lower-right part of Fig. 1), respectively. The fact that both these regions can stretch so far from the $\omega_{BL} \sim \sigma$ diagonal has to do with the fact that in neither of the two cases the subdominant VEV plays any significant role. This is quite clear for $\omega_{BL} < \sigma$ because in such a situation none of the scalar masses is governed by ω_{BL} while in the opposite case (i.e., for $\sigma < \omega_{BL}$) the lower VEV governs only SM-singlet (scalar) states which do not affect the evolution of the SM gauge couplings.

Let us also notice that the difference between the latter case and the breaking pattern (9) based on the two matching scales $\mu_{1,2}$ is just formal because the short hierarchy between the heavier states driven by ω_{BL} and those that decouple at σ is well accounted for by the threshold corrections in the matching equation (29).

2. Color octet scalar mass bounds

Turning our attention to the allowed range for the mass of the light colored octet scalar H_8 , the most general situation is depicted in Fig. 2. We see that the two-loop effects, as well as the improved implementation of the proton lifetime limits shrink the formerly identified range (see Fig. 6 in ref. [6]) by about four orders of magnitude. Hence, the overall consistency of the minimal $SO(10)$ GUT, together with the present day bounds on the matter stability, requires H_8 to be lighter than about 2000 TeV. Remarkably enough, this limit gets further reduced to about 20 TeV if no proton decay is detected up to a time scale of 2×10^{35} years corresponding to the maximum foreseen Hyper-Kamiokande reach, cf. Eq. (35).

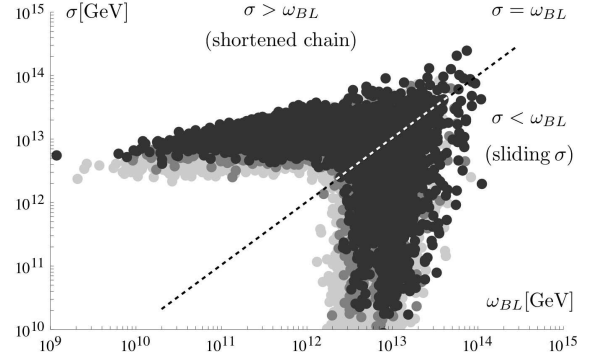


FIG. 1. The $|\omega_{BL}| - \sigma$ plane depicting the allowed part of the parameter space that supports a consistent two-loop gauge unification with a color octet scalar in the TeV domain (color code defined in Sect. IIB 2 a). For efficiency reasons, we reject all points that, in the one-loop approximation, yield σ below 10^{10} GeV; this leads to a reduction of the plot density in the uninteresting lowest σ region at two loops.

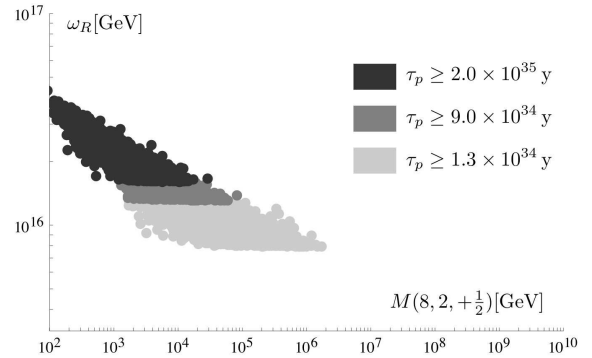


FIG. 2. The H_8 mass range allowed by the two-loop unification constraints and matter stability bounds. The present day bound on matter stability sets an upper bound on the H_8 mass of about 2000 TeV. The blurry lower-left boundary of the allowed region is an artefact of the numerical procedure in which, for efficiency reasons, we dump all uninteresting points with σ below 10^{10} GeV at one-loop. On the other hand, the upper-right boundary (which is the one that sets the stringent limit on the mass of H_8) corresponding to the sharp upper cut in Fig. 1 is enforced by the unification constraints and, as such, it is a robust feature of the model.

Note also that these bounds are robust with respect to the cuts imposed on the $B - L$ scale σ , as discussed in Sect. IIB 3. By looking at Fig. 3 we see that increasing σ does not affect the color octet mass upper limit (i.e., the rightmost points of a given color); the reason is that these points lay in the uppermost part of Fig. 1 and, as such, they are the last ones to be affected by additional constraints on σ . Nevertheless, the whole allowed region is eventually wiped out for $\sigma \gtrsim 2 \times 10^{14}$ GeV which sets a hard upper limit on the seesaw scale in this scenario.

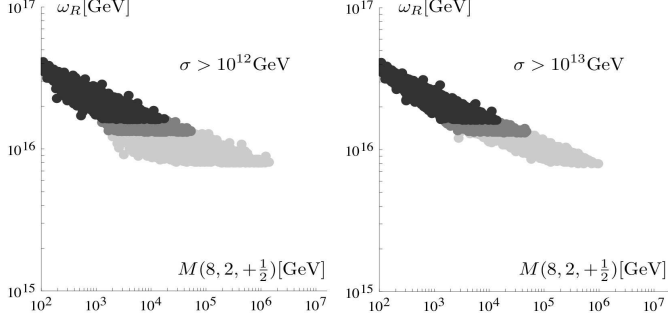


FIG. 3. The same as in Fig. 2 with the inclusion of the $B-L$ scale limits specified in Sect. II B 3 (namely, $\sigma \gtrsim 10^{12}$ GeV on the left and $\sigma \gtrsim 10^{13}$ GeV on the right). Since these constraints affect the bottom-left parts of the allowed regions, they preserve the upper limits quoted in Sect. II C 2. In all cases H_8 turns out to be lighter than about 2000 TeV. The bound shrinks to about 20 TeV for a proton lifetime above 10^{35} years (black area).

3. A specific example

For the sake of illustration, let us detail a specific solution corresponding to one of the black points in Figs. 1-3 (i.e., those with the proton lifetime exceeding 2×10^{35} years). The parameter-space coordinates of this sample point are given in TABLE I, the full breakdown of the bosonic part of the corresponding spectrum is given in TABLE II in Appendix A and, finally, the gauge unification pattern is depicted in Fig. 4.

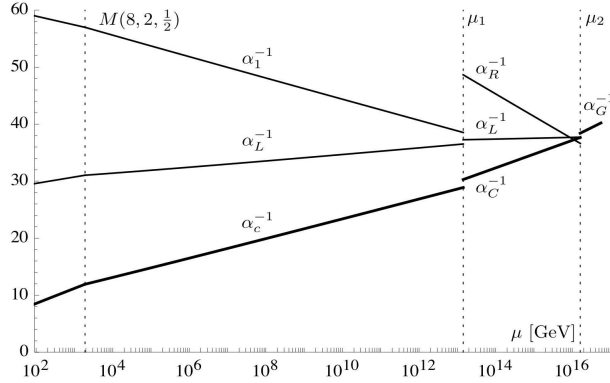


FIG. 4. A sample two-loop gauge unification pattern corresponding to one of the allowed solutions in Figs. 1, 2 and 3, see TABLE I and II for further details. The gauge running proceeds through four stages corresponding from top down to the $SO(10)$, $SU(4)_C \otimes SU(2)_L \otimes U(1)_R$, the $SM+H_8$ and, finally, the pure SM settings. The visible discontinuities in the non-Abelian gauge couplings at the upper two matching points are due to the large threshold corrections generated by the states decoupled at each scale.

Parameter	Value
ω_R	1.62×10^{16} GeV
ω_{BL}	5.41×10^{11} GeV
σ	-1.43×10^{13} GeV
a_0	0.74
α	-0.53
β_4	0.65
β'_4	-0.47
γ_2	0.09
λ_0	-0.36
λ_2	0.33
λ_4	0.62
λ'_4	0.41
$M(8, 2, +\frac{1}{2})$	1.90×10^3 GeV

TABLE I. Parameters underpinning the sample spectrum given in TABLE II in Appendix A with the corresponding unification pattern depicted in Fig. 4. The value of the τ parameter can be obtained from the requirement that the color octet scalar has the mass specified in the last row.

4. Further comments and consistency checks

a. Robustness of the two-loop renormalization group analysis. In order to verify the robustness of our numerical results we checked that, for a given set of the GUT-scale initial conditions, the results of the two-loop renormalization group analysis are only marginally depending on the particular choice of the matching scales $\mu_{1,2}$ in the vicinity of the main decoupling thresholds. As an example, by varying μ_i 's by as much as a factor of 3 leads to just minuscule variations in the low-energy values of α_i 's; by defining $\Delta_i \equiv \alpha_i^{-1}(M_Z)_{\text{perturbed}} - \alpha_i^{-1}(M_Z)_{\text{reference}}$, where the latter corresponds to the “standard” choice of μ_i 's as in Eq (10), we obtain $|\Delta_1 - \Delta_2| \lesssim 0.01$ and $|\Delta_2 - \Delta_3| \lesssim 0.1$.⁵

b. Effect of an extra 10_H in the Higgs sector. Concerning the impact of the so far neglected extra 10-dimensional scalar representations that represent a minimal extra measure in order to arrange a potentially viable flavor pattern (cf. Sect. III A) there is actually no need to undertake the technically demanding task of adding 10_H into the scalar potential (1) and redoing the same analysis from scratch. It is clear that its colored triplet components (cf. TABLE III) mix heavily with the other colored triplets in the potential and, thus, they live near to or at the GUT scale. Hence, the leading RGE effect of an additional 10_H comes from the need to mix its doublet component $(1, 2, \frac{1}{2})_{10}$ with $(15, 2, \frac{1}{2})_{126}$ in order to provide the right SM flavor structure. Such a mixing can

⁵ These numbers can be compared for instance with the low-energy uncertainties in Eq. (20), yielding $\Delta(\alpha_1^{-1}) \approx 0.014$, $\Delta(\alpha_2^{-1}) \approx 0.018$ and $\Delta(\alpha_3^{-1}) \approx 0.051$.

be significant if and only if both these multiplets survive down to about the 421 breaking scale and, hence, the extra $(1, 2, \frac{1}{2})_{10}$ should be considered among the active states in the relevant part of Sect. II B 1 d.

In order to gauge the effect of such an extra $(1, 2, \frac{1}{2})_{10}$, we can take advantage of the results obtained in the simple framework based on the MSH. In this approach, one ignores the details of the scalar spectrum and assumes a simple clustering of the minimal set of scalars needed for the spontaneous symmetry breaking at each given scale. Having subtracted the “noise” of the detailed spread of the scalar spectrum, this approach allows us to assess (rather reliably) the effects of a given extra state at a desired stage of the gauge running. Such a simplified analysis shows that, for a fixed H_8 mass, the net effect of an extra $(1, 2, \frac{1}{2})$ running throughout the $4_C 2_L 1_R$ stage is a further decrease of the GUT scale, M_G , while increasing the seesaw scale, M_{B-L} . Quantitatively, for a $\mathcal{O}(\text{TeV})$ H_8 the inclusion of a weak doublet between M_G and M_{B-L} , results into a -10% and a $+75\%$ shift in M_G and in M_{B-L} , respectively.

The fact that for a fixed M_8 the GUT scale (proportional to ω_R) is slightly lowered makes the proton lifetime constraints more severe. Thus, with the extra doublet at play, the general upper limit on M_8 derived in the previous sections (see namely Fig. 2) can only get stronger. At the same time, the seesaw scale may be increased up to a factor two, but with essentially no effects on the light H_8 mass constraints (cf. Fig. 3). Considering a more realistic case with the doublet components of 10_H lying somewhere between μ_2 and μ_1 the net effect of the extra 10_H is further weakened.

c. $M_8 - M_G$ correlation. The $M_8 - M_G$ correlation in Fig. 2 can be qualitatively understood by noticing that: (i) the H_8 contribution to the one-loop beta functions is such that $a_3 > a_2 > a_1$ (cf. TABLE II); (ii) taking the variation of the matching condition at μ_1 , $\alpha_L^{-1} - \frac{2}{5}\alpha_C^{-1} = \frac{3}{5}\alpha_R^{-1}$ (cf. also Fig. 4), with respect to M_8 there is a partial cancellation on the left-hand side so that $\partial\alpha_R^{-1}/\partial M_8 \approx 0$. Thus, the value of the GUT scale depends predominantly on the convergence point of α_L and α_C . As a consequence, the fact that higher unification scales select lighter H_8 is just a geometrical consequence of $a_3 > a_2$. For a similar discussion of the correlation between the GUT scale and the mass of a light $(8, 2, \frac{1}{2})$ octet in $SU(5)$ models see, e.g., [17, 18, 21].

d. $\Delta\alpha_3(M_Z)$ uncertainty. Among the most prominent sources of systematic errors one should certainly quote the $\mathcal{O}(0.6\%)$ uncertainty in $\alpha_3(M_Z)$ [cf. Eq. (20)], which translates into a conservative $\mathcal{O}(10\%)$ uncertainty in the determination of the seesaw and the GUT scales. The latter is, in turn, responsible for a larger $\mathcal{O}(50\%)$ uncertainty in the upper bound on the H_8 mass, which is mainly due to the almost flat slope of the $M_8 - M_G$ mass correlation (cf. Fig. 2).

e. Planck-scale physics. Worth of mention is the general fragility of grand unifications with respect to the Planck-scale (M_{Pl}) effects which, given the proximity of

the GUT scale and M_{Pl} , may not be entirely negligible. Concerning their possible impact on, e.g., the proton lifetime estimates, the most important of effect is the Planck-scale induced violation of the canonical normalization of the SM gauge fields [75, 76] due to the higher-order corrections to the gauge kinetic term emerging already at the $d = 5$ level: $\mathcal{L}^{(5)} \ni \text{Tr}[F_{\mu\nu} H F^{\mu\nu}]/M_{Pl}$. Here H is any scalar in the theory which can couple to a pair of adjoint representations, i.e., any field appearing in the symmetric part of the decomposition of their tensor product. For a GUT-scale VEV of H , this induces a percent-level effect which, after a suitable redefinition of the gauge fields, leads to similar-size shifts in the GUT-scale matching conditions which, on the other hand, are comparable to the two-loop effects.

Remarkably, if the GUT-scale symmetry breaking in $SO(10)$ is triggered by the VEV of 45_H , this problem is absent because $\text{Tr}[F_{\mu\nu} 45_H F^{\mu\nu}] = 0$ due to the fact that 45 is not in the symmetric part of the $45 \otimes 45$ decomposition [recall that $(45 \otimes 45)_{\text{sym}} = 54 \oplus 210 \oplus 770$]. Thus, the minimal $SO(10)$ scheme with the adjoint-driven Higgs mechanism is uniquely robust with respect to this class of quantum gravity effects (see also the discussion in ref. [77]). This makes the symmetry-breaking analysis more reliable and, hence, admits in principle for a strong reduction of this type of theoretical uncertainties in the proton lifetime estimates.

III. FLAVOUR AND ELECTROWEAK OBSERVABLES

The low-energy phenomenology of a light $\mathcal{O}(\text{TeV})$ -scale color octet scalar which couples directly to the quarks and the Higgs boson is severely constrained by the flavor and electroweak precision observables. In this section we describe such constraints from the point of view of the minimal $SO(10)$ GUT.

A. Tree-level FCNC

Color octet scalars with the same electroweak quantum numbers as the SM Higgs doublet have rather special properties since the suppression of the FCNC could naturally follow from the group structure and representation contents of the theory [13]. One possible way to achieve this is, indeed, imposing the minimal flavor violation (MFV) ansatz⁶ [78–80]. On the other hand,

⁶ The effective field theory approach to MFV consists in the assumptions that: (i) the full effective field theory is formally invariant under the $SU(3)^5$ flavor symmetry of the SM, and (ii) the SM Yukawas, which are promoted to spurion fields transforming under the $SU(3)^5$ symmetry, are the only irreducible sources of flavor breaking. Under these assumptions, only the scalars with the SM quantum numbers $(1, 2, +\frac{1}{2})$ and $(8, 2, +\frac{1}{2})$ can couple

the $SO(10)$ symmetry provides nontrivial constraints on the flavor sector of the effective SM+ H_8 theory. As we shall see, the analysis of the relevant structure reveals the existence of an intrinsic flavor-protection mechanism even without any additional “horizontal” assumption like MFV.

In order to proceed further we need to specify the $SO(10)$ Yukawa sector. At this stage, we shall consider two minimal, albeit rather different, realizations of the Yukawa sector which can potentially reproduce the pattern of fermion masses and mixings.⁷ Adding a complex⁸ 10_H representation into the Yukawa sector and focussing only on the mass sum-rules for the up- and down-quark mass matrices we have the following:

- Minimal field content [6],

$$M_U = Y'_{10} v_d^{*10}, \quad (36)$$

$$M_D = Y_{10} v_d^{10} + Y_{126} v_d^{126}, \quad (37)$$

- Peccei-Quinn (PQ) symmetry [81],

$$M_U = Y_{10} v_u^{10} + Y_{126} v_u^{126}, \quad (38)$$

$$M_D = Y_{10} v_d^{10} + Y_{126} v_d^{126}, \quad (39)$$

where Y_{10} and Y_{126} are the usual $SO(10)$ Yukawa couplings while Y'_{10} is an extra Yukawa available in the non-supersymmetric models with a complex 10_H . The presence of $v_{u,d}$ in (38)-(39) indicates that there are two light Higgs doublets in the low-energy effective theory in the PQ case while there is just one Higgs doublet in the minimal scenario (36)-(37). Note also that all the Yukawa couplings above are symmetric in the flavor space due to the gauge structure of the relevant $SO(10)$ invariants.

The second option is related to the implementation of the PQ solution to the strong CP problem in $SO(10)$. The need for an invisible axion requires an additional Higgs representation in the potential [84–86], minimally a 16_H . In spite of that the PQ symmetry actually reduces the number of couplings in the scalar potential and in the Yukawa sector with respect to the first case. In addition to that, a viable dark matter (DM) candidate, the axion, is available [87]. It is worth recalling that a DM candidate can be devised in the “minimal” setting as well, albeit requiring an extreme fine-tuning [88].

Returning to the issue of the induced FCNCs, the interactions of H_8 with the quarks are dictated by the Y_{126}

matrix, namely

$$\begin{aligned} & Y_{126} 16_M 16_M 126_H^* + \text{h.c.} \\ & \supset Y_{126} (qu^c H_{8u} + qd^c H_{8d}) + \text{h.c.} \\ & \supset Y_{126} (qu^c c_\theta H_8 + qd^c s_\theta H_8^*) + \text{h.c.} \end{aligned} \quad (40)$$

Natural flavor conservation in the neutral currents then requires Y_{126} to be (almost) diagonal in the same basis as M_U^{diag} and M_D^{diag} .

Remarkably enough, in the PQ case [cf. Eqs. (38)–(39)] the FCNCs turn out to be V_{CKM} -suppressed due to the special flavor structure of the relevant Yukawa couplings. This can be intuitively understood as follows: $SO(10)$ enforces symmetric Yukawa matrices and hence $V_{uL} = V_{uR}$ and $V_{dL} = V_{dR}$ where $V_{uL,R}$ and $V_{dL,R}$ denote the biunitary transformations which diagonalize the up- and down-quark mass matrices, respectively. Then, any flavor violation in the quark sector is encoded in the misalignment between V_{uL} and V_{dL} and, thus, the H_8 -mediated FCNCs are controlled by the CKM mixing matrix as in the MFV setting [20].

It is perhaps also worth noting that in the minimal case [cf. Eqs. (36)–(37)] the FCNCs are entirely absent if $[Y_{10}, Y_{126}] = 0$. The latter condition is not phenomenologically acceptable in the PQ setting since it would imply a diagonal CKM mixing matrix.

It is also important to stress that while Y_{126} is correlated to fermion masses and mixings, the angle θ (cf. Eq. (40)) is a function of a few scalar potential parameters [Eq. (B11) in [6]]. Thus, the couplings of H_8 to the fermions are quite constrained and the compatibility of a very light octet scalar with the flavor and electroweak (nonoblique) observables [13, 20], as, e.g., $K^0 - \bar{K}^0$ mixing, $B \rightarrow X_s \gamma$ and $Z \rightarrow b\bar{b}$, must be ultimately checked.

Needless to say, the PQ setting requires a detailed study of fermion masses and mixings, up to date missing to our knowledge. In particular, one must keep in mind that the orthogonality of the hypercharge and the PQ currents further constraints the VEVs of the light $H_{u,d}$ doublets by enforcing $v_u^2 = v_d^2$.

B. Custodial symmetry

The most crucial among the electroweak precision tests are those related to the breaking of the custodial symmetry⁹. Indeed, the Higgs VEV induces a tree-level mass splitting between the charged H_8^+ and neutral $H_8^{R,I}$ (real and imaginary) components of H_8 which determines a nonvanishing contribution to the T parameter [13]

$$\frac{\Delta m_{+,R}^2 \Delta m_{+,I}^2}{m_W^2 m_{+,R,I}^2} \approx 0.23 \Delta T, \quad (41)$$

to the quarks [13] and the amount of flavor violation beyond the SM is controlled by the standard Yukawas [20].

⁷ A complete and conclusive analysis on the viability of these settings in the $45_H \oplus 126_H$ model is still missing. For studies partially addressing the problem see e.g. [81–83].

⁸ The most minimal option of a real 10_H (enforcing $v_u^{10} = v_d^{*10}$) is not phenomenologically viable since it predicts a “wrong” GUT-scale mass relation $m_t \approx m_b$ [81].

⁹ Large contributions to the oblique parameter S can be easily avoided even for a sub-TeV-scale H_8 , while retaining at the same time a sizable impact on the SM $H \rightarrow \gamma\gamma$ rate [13].

where $\Delta m_{1,2}^2 \equiv m_1^2 - m_2^2$ and $m_{+,R,I}^2$ is the smallest among the masses. The approximate Eq. (41) holds with high accuracy even for $m_{+,R,I}$ as light as a few hundred GeV with Δm 's at the 100 GeV level. As a matter of fact the present experimental fits lead to $T = 0.02 \pm 0.11$ [89]; requiring a 1- σ saturation of T and taking $\Delta m_{+,R}^2 \approx \Delta m_{+,I}^2$ one obtains $\Delta m < 140$ GeV for the lightest mass of 300 GeV and $\Delta m < 250$ GeV for the lightest mass of 1 TeV. Since the mass splitting between the charged and neutral components is at most of the order of the electroweak scale such constraints can be naturally satisfied.

Large contributions to the T parameter can be also avoided when custodial symmetry limits in the parameter space of the Higgs doublet and H_8 effective scalar potential is considered¹⁰, albeit this generally requires fine-tuned relations among the scalar couplings. Though the embedding into $SO(10)$ could make such a limit non-trivial, a quantitative answer requires an extension of the $45_H \oplus 126_H$ scalar potential analyzed in [6], including those representations which are needed for a realistic description of fermion masses and mixings and have a nonzero projection on the Higgs doublets, like, e.g., a (complex) 10_H . This, however, is beyond the scope of the present work.

Finally, let us comment on the current experimental limits on the H_8 mass obtained namely from the direct LHC searches. While the recent experimental analysis based on dijet pair signatures [90, 91] exclude H_8 masses up to about 2 TeV, the low-energy window 200 – 320 GeV is not yet ruled out due to a gap in sensitivity to the soft jets [42]. On the other hand, the most recent four-jet final-state studies of the ATLAS [92] and CMS [93] collaborations seem to exclude also this range.

IV. CONCLUSIONS

As emphasised recently a light (sub-TeV) colored octet scalar may help in explaining the $H \rightarrow \gamma\gamma$ anomaly still present in the LHC data. In a preceding paper we scrutinized the role of intermediate-scale colored scalar states in the minimal $SO(10)$ grand unification. The presence of such states together with the unification constraints and the associated large threshold effects allow for the scale of the $B - L$ breaking in the desired ballpark for the neutrino mass generation via standard seesaw. Moreover, the model may be prone to future experimental testability due to a relatively rapid proton decay inherent to this class of scenarios¹¹.

¹⁰ See refs. [13, 30] for a detailed discussion of precision electroweak constraints on the scalar octet interactions.

¹¹ Another viable threshold configuration identified in [6] which allows for a large enough seesaw scale is that of an intermediate-scale color sextet scalar $(6, 3, +\frac{1}{3})$. Preliminary results indicate that two-loop effects further lower the GUT scale thus reducing the physically allowed domain of this class of solutions [94].

In this paper, we provide a significantly refined study of the setup with a light color octet scalar by including the leading two-loop gauge running effects together with a more detailed analysis of the proton decay width. Focusing on the interesting anticorrelation between the proton lifetime and the mass of the light H_8 we find that the present data on the matter stability require M_8 below about 2000 TeV; yet stronger limits at the level of few tens of TeV are expected if proton decay is not observed even at the next generation facilities. In all cases a sizeable fraction of the parameter space allows for H_8 masses within the reach of the LHC.

Acknowledgments

S. B. is partially supported by the italian MIUR Grant No. 2010YJ2NYW.001 and by the EU Marie Curie ITN UNILHC, Grant Agreement PITN-GA-2009-237920. The work of L. D. L. is supported by the DFG through the SFB/TR 9 “Computational Particle Physics.” In the initial phase, the work of M. M. was supported by the Marie Curie Intra European Fellowship within the 7th European Community Framework Programme FP7-PEOPLE-2009-IEF, Contract No. PIEF-GA-2009-253119; by the EU Network Grant No. UNILHC PITN-GA-2009-237920; by the Spanish MICINN Grants No. FPA2008-00319/FPA and No. MULTIDARK CAD2009-00064 (Consolider-Ingenio 2010 Programme); and by the Generalitat Valenciana Grant No. Prometeo/2009/091. In the later stages, M. M. was supported by the Marie Curie Career Integration Grant within the 7th European Community Framework Programme FP7-PEOPLE-2011-CIG, Contract No. PCIG10-GA-2011-303565; and by the Research Proposal No. MSM0021620859 of the Ministry of Education, Youth and Sports of the Czech Republic.

Appendix A: A sample scalar spectrum

Details of the scalar spectrum corresponding to the sample two-loop solution displayed in Fig. 4 are given in TABLE II. For the sake of brevity, for each multiplet Q therein we present only its contribution to the one-loop part of the gauge beta-function (Δa_Q) which is enough to reconstruct the $A_{SL,SR}$ factors (32) governing the one-loop evolution of the effective $d = 6$ proton decay operators and, hence, the proton partial width (31); in the sample case one has $\Gamma(p \rightarrow \pi^0 e^+) \approx (2.0 \times 10^{35} \text{ years})^{-1}$. In TABLE II, the acronyms CS, RS, VB, GB stay for complex scalars, real scalars, vector bosons and would-be Goldstone bosons, respectively.

Appendix B: One-loop matching

For completeness, we report the detailed form of the structures entering the matching of the gauge couplings at the $SO(10) - 4_C 2_L 1_R$ threshold μ_2 and at the $4_C 2_L 1_R - \text{SM} + H_8$ threshold μ_1 , respectively.

The $SO(10) \rightarrow 4_C 2_L 1_R$ matching at μ_2 :

$$\begin{aligned} \lambda_C = & \frac{1}{48\pi^2} \left[4 - 44 \log \frac{M(3, 2, +\frac{1}{6})_{\text{VB}}}{\mu_2} + 2 \log \frac{M(3, 2, +\frac{1}{6})_{\text{GB}}}{\mu_2} \right. \\ & - 44 \log \frac{M(3, 2, -\frac{5}{6})_{\text{VB}}}{\mu_2} + 2 \log \frac{M(3, 2, -\frac{5}{6})_{\text{GB}}}{\mu_2} \\ & + \log \frac{M(3, 1, +\frac{2}{3})_{\text{CS}}^{(2)}}{\mu_2} + \log \frac{M(3, 1, -\frac{4}{3})_{\text{CS}}}{\mu_2} \\ & + 2 \log \frac{M(3, 2, +\frac{1}{6})_{\text{CS}}^{(2)}}{\mu_2} + 2 \log \frac{M(3, 2, +\frac{7}{6})_{\text{CS}}^{(2)}}{\mu_2} \\ & + \log \frac{M(3, 1, +\frac{1}{3})_{\text{CS}}^{(1)}}{\mu_2} + \log \frac{M(3, 1, +\frac{1}{3})_{\text{CS}}^{(2)}}{\mu_2} \\ & + \log \frac{M(3, 1, +\frac{1}{3})_{\text{CS}}^{(3)}}{\mu_2} + 3 \log \frac{M(3, 3, +\frac{1}{3})_{\text{CS}}}{\mu_2} \\ & + 5 \log \frac{M(6, 1, +\frac{1}{3})_{\text{CS}}}{\mu_2} + 5 \log \frac{M(6, 1, -\frac{2}{3})_{\text{CS}}}{\mu_2} \\ & + 15 \log \frac{M(6, 3, -\frac{1}{3})_{\text{CS}}}{\mu_2} + 3 \log \frac{M(8, 1, 0)_{\text{RS}}}{\mu_2} \\ & \left. + 12 \log \frac{M(8, 2, +\frac{1}{2})_{\text{CS}}^{(2)}}{\mu_2} \right], \end{aligned}$$

$$\begin{aligned} \lambda_L = & \frac{1}{48\pi^2} \left[6 - 66 \log \frac{M(3, 2, +\frac{1}{6})_{\text{VB}}}{\mu_2} + 3 \log \frac{M(3, 2, +\frac{1}{6})_{\text{GB}}}{\mu_2} \right. \\ & - 66 \log \frac{M(3, 2, -\frac{5}{6})_{\text{VB}}}{\mu_2} + 3 \log \frac{M(3, 2, -\frac{5}{6})_{\text{GB}}}{\mu_2} \\ & + 3 \log \frac{M(3, 2, +\frac{1}{6})_{\text{CS}}^{(2)}}{\mu_2} + 3 \log \frac{M(3, 2, +\frac{7}{6})_{\text{CS}}^{(2)}}{\mu_2} \\ & + 12 \log \frac{M(3, 3, +\frac{1}{3})_{\text{CS}}}{\mu_2} + 4 \log \frac{M(1, 3, +1)_{\text{CS}}}{\mu_2} \\ & + \frac{1}{2} \log \frac{M(1, 2, +\frac{1}{2})_{\text{RS}}^{(1)}}{\mu_2} + \frac{1}{2} \log \frac{M(1, 2, +\frac{1}{2})_{\text{RS}}^{(2)}}{\mu_2} \\ & + 24 \log \frac{M(6, 3, -\frac{1}{3})_{\text{CS}}}{\mu_2} + 2 \log \frac{M(1, 3, 0)_{\text{RS}}}{\mu_2} \\ & \left. + 8 \log \frac{M(8, 2, +\frac{1}{2})_{\text{CS}}^{(2)}}{\mu_2} \right], \end{aligned}$$

$$\begin{aligned} \lambda_R = & \frac{1}{48\pi^2} \left[8 - 44 \log \frac{M(1, 1, +1)_{\text{VB}}}{\mu_2} + 2 \log \frac{M(1, 1, +1)_{\text{GB}}}{\mu_2} \right. \\ & - 66 \log \frac{M(3, 2, +\frac{1}{6})_{\text{VB}}}{\mu_2} + 3 \log \frac{M(3, 2, +\frac{1}{6})_{\text{GB}}}{\mu_2} \\ & - 66 \log \frac{M(3, 2, -\frac{5}{6})_{\text{VB}}}{\mu_2} + 3 \log \frac{M(3, 2, -\frac{5}{6})_{\text{GB}}}{\mu_2} \\ & + 3 \log \frac{M(3, 2, +\frac{1}{6})_{\text{CS}}^{(2)}}{\mu_2} + 3 \log \frac{M(3, 2, +\frac{7}{6})_{\text{CS}}^{(2)}}{\mu_2} \\ & + \frac{1}{2} \log \frac{M(1, 2, +\frac{1}{2})_{\text{RS}}^{(1)}}{\mu_2} + \frac{1}{2} \log \frac{M(1, 2, +\frac{1}{2})_{\text{RS}}^{(2)}}{\mu_2} \\ & + 12 \log \frac{M(6, 1, -\frac{2}{3})_{\text{CS}}}{\mu_2} + 8 \log \frac{M(8, 2, +\frac{1}{2})_{\text{CS}}^{(2)}}{\mu_2} \\ & \left. + 6 \log \frac{M(3, 1, -\frac{4}{3})_{\text{CS}}}{\mu_2} + 2 \log \frac{M(1, 1, -2)_{\text{CS}}}{\mu_2} \right]. \end{aligned}$$

The $4_C 2_L 1_R \rightarrow 3_c 2_L 1_R 1_X \rightarrow 3_c 2_L 1_Y$ matching at μ_1 :

$$\begin{aligned} \lambda_c = & \frac{1}{48\pi^2} \left[1 - 22 \log \frac{M(3, 1, +\frac{2}{3})_{\text{VB}}}{\mu_1} + \log \frac{M(3, 1, +\frac{2}{3})_{\text{GB}}}{\mu_1} \right. \\ & + 2 \log \frac{M(3, 2, +\frac{1}{6})_{\text{CS}}^{(3)}}{\mu_1} + 2 \log \frac{M(3, 2, +\frac{7}{6})_{\text{CS}}}{\mu_1} \\ & \left. + 5 \log \frac{M(6, 1, +\frac{4}{3})_{\text{CS}}}{\mu_1} \right], \end{aligned}$$

$$\lambda_L = \frac{1}{16\pi^2} \left[\log \frac{M(3, 2, +\frac{1}{6})_{\text{CS}}^{(3)}}{\mu_1} + \log \frac{M(3, 2, +\frac{7}{6})_{\text{CS}}}{\mu_1} \right],$$

$$\begin{aligned} \lambda_{RR} = & \frac{1}{48\pi^2} \left[2 \log \frac{M(1, 1, 0)_{\text{GB}}}{\mu_1} + 6 \log \frac{M(3, 1, +\frac{2}{3})_{\text{GB}}}{\mu_1} \right. \\ & + 3 \log \frac{M(3, 2, +\frac{1}{6})_{\text{CS}}^{(3)}}{\mu_1} + 3 \log \frac{M(3, 2, +\frac{7}{6})_{\text{CS}}}{\mu_1} \\ & \left. + 12 \log \frac{M(6, 1, +\frac{4}{3})_{\text{CS}}}{\mu_1} \right], \end{aligned}$$

$$\begin{aligned} \lambda_{RX} = \lambda_{XR} = & -\frac{1}{8\sqrt{6}\pi^2} \left[\log \frac{M(1, 1, 0)_{\text{GB}}}{\mu_1} \right. \\ & + \log \frac{M(3, 1, +\frac{2}{3})_{\text{GB}}}{\mu_1} - 2 \log \frac{M(6, 1, +\frac{4}{3})_{\text{CS}}}{\mu_1} \\ & \left. + 2 \log \frac{M(3, 2, +\frac{1}{6})_{\text{CS}}^{(3)}}{\mu_1} + 2 \log \frac{M(3, 2, +\frac{7}{6})_{\text{CS}}}{\mu_1} \right], \end{aligned}$$

$$\begin{aligned} \lambda_{XX} = & \frac{1}{48\pi^2} \left[4 - 88 \log \frac{M(3, 1, +\frac{2}{3})_{\text{VB}}}{\mu_1} + \log \frac{M(3, 1, +\frac{2}{3})_{\text{GB}}}{\mu_1} \right. \\ & + 8 \log \frac{M(3, 2, +\frac{1}{6})_{\text{CS}}^{(3)}}{\mu_1} + 8 \log \frac{M(3, 2, +\frac{7}{6})_{\text{CS}}}{\mu_1} \\ & \left. + 2 \log \frac{M(6, 1, +\frac{4}{3})_{\text{CS}}}{\mu_1} + 3 \log \frac{M(1, 1, 0)_{\text{GB}}}{\mu_1} \right]. \end{aligned}$$

A few comments are in order. First, a generic analytic identification of the hierarchy of the mass-eigenstates of the mass matrices larger than 2×2 is very difficult due to possible accidental cancellations and, thus, in some cases, the actual mass ordering of the eigenstates labeled by $1, 2, 3, \dots$ in the third column of TABLE II may be different than what is expected from the ordering in the formulas above (where the different eigenstates are labeled by superscripts).¹² Although this may look contrived, it is readily verified that to a very good accuracy the only effect of such a “misidentification” is an overall shift of some of the “segments” of the gauge running curves between μ_2 and μ_1 in figures like Fig. 4, with a negligible effect on the low-energy values of the gauge couplings.¹³

Second, we may further simplify the matching formulas by taking advantage of the fact that in the Feynman gauge the masses of the Goldstones equal those of the corresponding vectors; hence, the contributions from these two sources can be collapsed into a single log term.

Finally, a comment on the artificial “reality” of the two SM-Higgs scalars $(1, 2, +\frac{1}{2})_{\text{RS}}^{(1,2)}$ entering the formulas for $\lambda_{L,R}$ at the μ_2 matching scale. As a matter of fact, besides the lightest eigenstate playing the role of the SM Higgs doublet, all the heavy complex $(1, 2, +\frac{1}{2})_{\text{CS}}^{(i)}$ eigenstates of the relevant doublet mass matrix should be integrated out at μ_2 . However, the spectrum of the doublet-like scalars is unavailable unless all the extra scalars, required for a realistic Yukawa sector (minimally, a complex 10_H ; cf. also Sect. III A), are consistently taken into account.

Fortunately, such a detailed study is not needed as one can approximate the effect of a light complex doublet by “averaging” over the eigenvalues of the 2×2 doublet mass matrix in the $45_H \oplus 126_H$ sector, namely by taking the two “heavy” doublets as real fields so that the heavy doublet degrees of freedom are counted correctly. As rough as it may sound conceptually, this “escamotage” has essentially no effect on the numerical results due to the generally very small impact of the scalar doublets on the evolution of the gauge couplings as well as on the associated threshold corrections. The interested reader can find a more detailed discussion of these issues in Section II C 4 b and in ref. [6].

Appendix C: $SO(10)$ Higgs representations

The decomposition of the 10_H , 45_H and 126_H representations with respect to all relevant intermediate symmetries is detailed in TABLES III, IV and V.

Multiplet Q	Type	Eigenstate	Δa_Q	Mass [GeV]
$(8, 2, +\frac{1}{2})$	CS	1	$(2, \frac{4}{3}, \frac{4}{5})$	1.9×10^3
$(\bar{3}, 1, -\frac{2}{3})$	VB	1	$(-\frac{11}{6}, 0, -\frac{44}{15})$	1.2×10^{13}
$(3, 1, +\frac{2}{3})$	VB	1	$(-\frac{11}{6}, 0, -\frac{44}{15})$	1.2×10^{13}
$(\bar{3}, 1, -\frac{2}{3})$	GB	1	$(\frac{1}{6}, 0, \frac{4}{15})$	1.2×10^{13}
$(1, 1, 0)$	VB	1	$(0, 0, 0)$	2.7×10^{13}
$(1, 1, 0)$	GB	1	$(0, 0, 0)$	2.7×10^{13}
$(3, 2, +\frac{1}{6})$	CS	2	$(\frac{1}{3}, \frac{1}{2}, \frac{1}{30})$	8.2×10^{13}
$(3, 2, +\frac{7}{6})$	CS	1	$(\frac{1}{3}, \frac{1}{2}, \frac{49}{30})$	1.1×10^{14}
$(1, 2, +\frac{1}{2})$	RS	1	$(0, \frac{1}{12}, \frac{1}{20})$	1.1×10^{14}
$(1, 1, 0)$	RS	2	$(0, 0, 0)$	4.2×10^{15}
$(\bar{3}, 1, -\frac{2}{3})$	CS	2	$(\frac{1}{6}, 0, \frac{4}{15})$	4.2×10^{15}
$(\bar{6}, 1, -\frac{4}{3})$	CS	1	$(\frac{5}{6}, 0, \frac{32}{15})$	5.4×10^{15}
$(1, 1, 0)$	RS	3	$(0, 0, 0)$	5.4×10^{15}
$(8, 1, 0)$	RS	1	$(\frac{1}{2}, 0, 0)$	6.2×10^{15}
$(6, 3, +\frac{1}{3})$	CS	1	$(\frac{5}{2}, 4, \frac{2}{5})$	7.4×10^{15}
$(3, 3, -\frac{1}{3})$	CS	1	$(\frac{1}{2}, 2, \frac{1}{5})$	7.4×10^{15}
$(1, 3, -1)$	CS	1	$(0, \frac{2}{3}, \frac{3}{5})$	7.4×10^{15}
$(1, 3, 0)$	RS	1	$(0, \frac{1}{3}, 0)$	8.4×10^{15}
$(\bar{3}, 2, +\frac{5}{6})$	VB	1	$(-\frac{11}{3}, -\frac{11}{2}, -\frac{55}{6})$	9.7×10^{15}
$(3, 2, -\frac{5}{6})$	VB	1	$(-\frac{11}{3}, -\frac{11}{2}, -\frac{55}{6})$	9.7×10^{15}
$(3, 2, -\frac{5}{6})$	GB	1	$(\frac{1}{3}, \frac{1}{2}, \frac{5}{6})$	9.7×10^{15}
$(\bar{3}, 2, -\frac{1}{6})$	VB	1	$(-\frac{11}{3}, -\frac{11}{2}, -\frac{11}{30})$	9.7×10^{15}
$(3, 2, +\frac{1}{6})$	VB	1	$(-\frac{11}{3}, -\frac{11}{2}, -\frac{11}{30})$	9.7×10^{15}
$(3, 2, +\frac{1}{6})$	GB	1	$(\frac{1}{3}, \frac{1}{2}, \frac{1}{30})$	9.7×10^{15}
$(\bar{3}, 1, +\frac{1}{3})$	CS	1	$(\frac{1}{6}, 0, \frac{1}{15})$	1.2×10^{16}
$(\bar{3}, 1, +\frac{1}{3})$	CS	2	$(\frac{1}{6}, 0, \frac{1}{15})$	1.8×10^{16}
$(1, 1, -1)$	VB	1	$(0, 0, -\frac{11}{5})$	1.9×10^{16}
$(1, 1, +1)$	VB	1	$(0, 0, -\frac{11}{5})$	1.9×10^{16}
$(1, 1, +1)$	GB	1	$(0, 0, \frac{1}{5})$	1.9×10^{16}
$(1, 1, +1)$	CS	2	$(0, 0, \frac{1}{5})$	2.0×10^{16}
$(\bar{3}, 1, +\frac{1}{3})$	CS	3	$(\frac{1}{6}, 0, \frac{1}{15})$	2.0×10^{16}
$(\bar{6}, 1, -\frac{1}{3})$	CS	1	$(\frac{5}{6}, 0, \frac{2}{15})$	2.0×10^{16}
$(3, 2, +\frac{7}{6})$	CS	2	$(\frac{1}{3}, \frac{1}{2}, \frac{49}{30})$	2.3×10^{16}
$(1, 2, +\frac{1}{2})$	RS	2	$(0, \frac{1}{12}, \frac{1}{20})$	2.3×10^{16}
$(8, 2, +\frac{1}{2})$	CS	2	$(2, \frac{4}{3}, \frac{4}{5})$	2.3×10^{16}
$(3, 2, +\frac{1}{6})$	CS	3	$(\frac{1}{3}, \frac{1}{2}, \frac{1}{30})$	2.3×10^{16}
$(1, 1, +2)$	CS	1	$(0, 0, \frac{4}{5})$	3.3×10^{16}
$(\bar{3}, 1, +\frac{4}{3})$	CS	1	$(\frac{1}{6}, 0, \frac{16}{15})$	3.3×10^{16}
$(\bar{6}, 1, +\frac{2}{3})$	CS	1	$(\frac{5}{6}, 0, \frac{8}{15})$	3.3×10^{16}
$(1, 1, 0)$	RS	4	$(0, 0, 0)$	5.6×10^{16}

TABLE II. A sample spectrum featuring a light $(8, 2, +\frac{1}{2})$ multiplet. The relevant scalar potential parameters are given in TABLE I. Δa_Q indicate the shifts in the one-loop beta-function entering formula (31) due to a given multiplet Q . The light threshold and the vector bosons defining the GUT scale are in boldface. As a consistency check, $a_{SM} + \sum \Delta a_Q = (-\frac{37}{3}, -\frac{37}{3}, -\frac{37}{3})$.

¹² Notice, for instance, that in the specific example in TABLE II the mass of $M(3, 2, +\frac{1}{6})_{\text{CS}}^{(2)}$ entering the matching factor λ_C at

μ_2 is smaller than $M(3, 2, +\frac{1}{6})_{\text{CS}}^{(3)}$ entering λ_c at μ_1 .

¹³ Indeed, $\log M_A/\mu_1 + \log M_B/\mu_2 = \log M_A/\mu_2 + \log M_B/\mu_1$.

$4_C 2_L 2_R$	$4_C 2_L 1_R$	$3_c 2_L 2_R 1_{BL}$	$3_c 2_L 1_R 1_{BL}$	$3_c 2_L 1_Y$	$5 1_Z$	$5' 1_{Z'}$
$(6, 1, 1)$	$(6, 1, 0)$	$(3, 1, 1, -\frac{2}{3})$	$(3, 1, 0, -\frac{2}{3})$	$(3, 1, -\frac{1}{3})$	$(5, -2)$	$(5, -2)$
		$(\bar{3}, 1, 1, +\frac{2}{3})$	$(\bar{3}, 1, 0, +\frac{2}{3})$	$(\bar{3}, 1, +\frac{1}{3})$	$(\bar{5}, +2)$	$(\bar{5}, +2)$
$(1, 2, 2)$	$(1, 2, +\frac{1}{2})$	$(1, 2, 2, 0)$	$(1, 2, +\frac{1}{2}, 0)$	$(1, 2, +\frac{1}{2})$	$(5, -2)$	$(5, +2)$
	$(1, 2, -\frac{1}{2})$		$(1, 2, -\frac{1}{2}, 0)$	$(1, 2, -\frac{1}{2})$	$(\bar{5}, +2)$	$(\bar{5}, -2)$

TABLE III. Decomposition of the fundamental representation 10 with respect to the various $SO(10)$ subgroups. The definitions and normalization of the abelian charges are given in Sect. II.

$4_C 2_L 2_R$	$4_C 2_L 1_R$	$3_c 2_L 2_R 1_{BL}$	$3_c 2_L 1_R 1_{BL}$	$3_c 2_L 1_Y$	$5 1_Z$	$5' 1_{Z'}$
$(1, 1, 3)$	$(1, 1, +1)$	$(1, 1, 3, 0)$	$(1, 1, +1, 0)$	$(1, 1, +1)$	$(10, -4)$	$(\bar{10}, +4)$
	$(1, 1, 0)$		$(1, 1, 0, 0)$	$(1, 1, 0)$	$(1, 0)$	$(1, 0)$
	$(1, 1, -1)$		$(1, 1, -1, 0)$	$(1, 1, -1)$	$(\bar{10}, +4)$	$(10, -4)$
$(1, 3, 1)$	$(1, 3, 0)$	$(1, 3, 1, 0)$	$(1, 3, 0, 0)$	$(1, 3, 0)$	$(24, 0)$	$(24, 0)$
$(6, 2, 2)$	$(6, 2, +\frac{1}{2})$	$(3, 2, 2, -\frac{2}{3})$	$(3, 2, +\frac{1}{2}, -\frac{2}{3})$	$(3, 2, +\frac{1}{6})$	$(10, -4)$	$(24, 0)$
	$(6, 2, -\frac{1}{2})$		$(3, 2, -\frac{1}{2}, -\frac{2}{3})$	$(3, 2, -\frac{5}{6})$	$(24, 0)$	$(10, -4)$
		$(\bar{3}, 2, 2, +\frac{2}{3})$	$(\bar{3}, 2, +\frac{1}{2}, +\frac{2}{3})$	$(\bar{3}, 2, +\frac{5}{6})$	$(24, 0)$	$(\bar{10}, +4)$
			$(\bar{3}, 2, -\frac{1}{2}, +\frac{2}{3})$	$(\bar{3}, 2, -\frac{1}{6})$	$(\bar{10}, +4)$	$(24, 0)$
$(15, 1, 1)$	$(15, 1, 0)$	$(1, 1, 1, 0)$	$(1, 1, 0, 0)$	$(1, 1, 0)$	$(24, 0)$	$(24, 0)$
		$(3, 1, 1, +\frac{4}{3})$	$(3, 1, 0, +\frac{4}{3})$	$(3, 1, +\frac{2}{3})$	$(\bar{10}, +4)$	$(\bar{10}, +4)$
		$(\bar{3}, 1, 1, -\frac{4}{3})$	$(\bar{3}, 1, 0, -\frac{4}{3})$	$(\bar{3}, 1, -\frac{2}{3})$	$(10, -4)$	$(10, -4)$
		$(8, 1, 1, 0)$	$(8, 1, 0, 0)$	$(8, 1, 0)$	$(24, 0)$	$(24, 0)$

TABLE IV. Same as in TABLE III for the 45 representation.

$4_C 2_L 2_R$	$4_C 2_L 1_R$	$3_c 2_L 2_R 1_{BL}$	$3_c 2_L 1_R 1_{BL}$	$3_c 2_L 1_Y$	$5 1_Z$	$5' 1_{Z'}$
$(6, 1, 1)$	$(6, 1, 0)$	$(\bar{3}, 1, 1, +\frac{2}{3})$	$(\bar{3}, 1, 0, +\frac{2}{3})$	$(\bar{3}, 1, +\frac{1}{3})$	$(\bar{5}, +2)$	$(\bar{5}, +2)$
		$(3, 1, 1, -\frac{2}{3})$	$(3, 1, 0, -\frac{2}{3})$	$(3, 1, -\frac{1}{3})$	$(45, -2)$	$(45, -2)$
$(10, 3, 1)$	$(10, 3, 0)$	$(1, 3, 1, -2)$	$(1, 3, 0, -2)$	$(1, 3, -1)$	$(\bar{15}, -6)$	$(\bar{15}, -6)$
		$(3, 3, 1, -\frac{2}{3})$	$(3, 3, 0, -\frac{2}{3})$	$(3, 3, -\frac{1}{3})$	$(45, -2)$	$(45, -2)$
		$(6, 3, 1, +\frac{2}{3})$	$(6, 3, 0, +\frac{2}{3})$	$(6, 3, +\frac{1}{3})$	$(\bar{50}, +2)$	$(\bar{50}, +2)$
$(\bar{10}, 1, 3)$	$(\bar{10}, 1, -1)$	$(1, 1, 3, +2)$	$(1, 1, -1, +2)$	$(1, 1, 0)$	$(1, +10)$	$(\bar{50}, +2)$
	$(\bar{10}, 1, 0)$		$(1, 1, 0, +2)$	$(1, 1, +1)$	$(10, +6)$	$(10, +6)$
	$(\bar{10}, 1, +1)$		$(1, 1, +1, +2)$	$(1, 1, +2)$	$(\bar{50}, +2)$	$(1, +10)$
		$(\bar{3}, 1, 3, +\frac{2}{3})$	$(\bar{3}, 1, -1, +\frac{2}{3})$	$(\bar{3}, 1, -\frac{2}{3})$	$(10, +6)$	$(45, -2)$
			$(\bar{3}, 1, 0, +\frac{2}{3})$	$(\bar{3}, 1, +\frac{1}{3})$	$(\bar{50}, +2)$	$(\bar{50}, +2)$
			$(\bar{3}, 1, +1, +\frac{2}{3})$	$(\bar{3}, 1, +\frac{4}{3})$	$(45, -2)$	$(10, +6)$
		$(\bar{6}, 1, 3, -\frac{2}{3})$	$(\bar{6}, 1, -1, -\frac{2}{3})$	$(\bar{6}, 1, -\frac{4}{3})$	$(\bar{50}, +2)$	$(\bar{15}, -6)$
			$(\bar{6}, 1, 0, -\frac{2}{3})$	$(\bar{6}, 1, -\frac{1}{3})$	$(45, -2)$	$(45, -2)$
			$(\bar{6}, 1, +1, -\frac{2}{3})$	$(\bar{6}, 1, +\frac{2}{3})$	$(\bar{15}, -6)$	$(\bar{50}, +2)$
$(15, 2, 2)$	$(15, 2, -\frac{1}{2})$	$(1, 2, 2, 0)$	$(1, 2, -\frac{1}{2}, 0)$	$(1, 2, -\frac{1}{2})$	$(\bar{5}, +2)$	$(45, -2)$
	$(15, 2, +\frac{1}{2})$		$(1, 2, +\frac{1}{2}, 0)$	$(1, 2, +\frac{1}{2})$	$(45, -2)$	$(\bar{5}, +2)$
		$(\bar{3}, 2, 2, -\frac{4}{3})$	$(\bar{3}, 2, -\frac{1}{2}, -\frac{4}{3})$	$(\bar{3}, 2, -\frac{7}{6})$	$(45, -2)$	$(\bar{15}, -6)$
			$(\bar{3}, 2, +\frac{1}{2}, -\frac{4}{3})$	$(\bar{3}, 2, -\frac{1}{6})$	$(\bar{15}, -6)$	$(45, -2)$
		$(3, 2, 2, +\frac{4}{3})$	$(3, 2, +\frac{1}{2}, +\frac{4}{3})$	$(3, 2, +\frac{7}{6})$	$(\bar{50}, +2)$	$(10, +6)$
			$(3, 2, -\frac{1}{2}, +\frac{4}{3})$	$(3, 2, +\frac{1}{6})$	$(10, +6)$	$(\bar{50}, +2)$
		$(8, 2, 2, 0)$	$(8, 2, -\frac{1}{2}, 0)$	$(8, 2, -\frac{1}{2})$	$(\bar{50}, +2)$	$(45, -2)$
			$(8, 2, +\frac{1}{2}, 0)$	$(8, 2, +\frac{1}{2})$	$(45, -2)$	$(\bar{50}, +2)$

TABLE V. Same as in TABLE III for the 126 representation.

-
- [1] M. Yasue, *Symmetry Breaking Of $So(10)$ And Constraints On Higgs Potential. 1. Adjoint (45) And Spinorial (16)*, Phys. Rev. D **24**, 1005 (1981).
- [2] G. Anastaze, J. P. Derendinger and F. Buccella, *Intermediate Symmetries In The $So(10)$ Model With (16+16) + 45 Higgses*, Z. Phys. C **20**, 269 (1983).
- [3] K. S. Babu and E. Ma, *Symmetry Breaking In $So(10)$: Higgs Boson Structure*, Phys. Rev. D **31**, 2316 (1985).
- [4] L. -F. Li, *Group Theory of the Spontaneously Broken Gauge Symmetries*, Phys. Rev. D **9**, 1723 (1974).
- [5] S. Bertolini, L. Di Luzio and M. Malinsky, *The vacuum of the minimal nonsupersymmetric $SO(10)$ unification*, Phys. Rev. D **81**, 035015 (2010) [arXiv:0912.1796 [hep-ph]].
- [6] S. Bertolini, L. Di Luzio and M. Malinsky, *Seesaw Scale in the Minimal Renormalizable $SO(10)$ Grand Unification*, Phys. Rev. D **85**, 095014 (2012) [arXiv:1202.0807 [hep-ph]].
- [7] S. Bertolini, L. Di Luzio, and M. Malinsky, *Intermediate mass scales in the nonsupersymmetric $SO(10)$ grand unification: A Reappraisal*, Phys. Rev. D **80**, 015013 (2009) [arXiv:0903.4049 [hep-ph]].
- [8] I. Dorsner, S. Fajfer, A. Greljo and J. F. Kamenik, *Higgs Uncovering Light Scalar Remnants of High Scale Matter Unification*, arXiv:1208.1266 [hep-ph].
- [9] M. Reece, *Vacuum Instabilities with a Wrong-Sign Higgs-Gluon-Gluon Amplitude*, arXiv:1208.1765 [hep-ph].
- [10] G. Aad *et al.* [ATLAS Collaboration], *Observation of a new particle in the search for the Standard Model Higgs boson with the ATLAS detector at the LHC*, Phys. Lett. B **716**, 1 (2012) [arXiv:1207.7214 [hep-ex]].
- [11] S. Chatrchyan *et al.* [CMS Collaboration], *Observation of a new boson at a mass of 125 GeV with the CMS experiment at the LHC*, Phys. Lett. B **716**, 30 (2012) [arXiv:1207.7235 [hep-ex]].
- [12] [ATLAS Collaboration], *Observation and study of the Higgs boson candidate in the two photon decay channel with the ATLAS detector at the LHC*, ATLAS-CONF-2012-168.
- [13] A. V. Manohar and M. B. Wise, *Flavor changing neutral currents, an extended scalar sector, and the Higgs production rate at the LHC*, Phys. Rev. D **74** (2006) 035009 [arXiv:hep-ph/0606172].
- [14] P. H. Frampton and S. L. Glashow, *Chiral Color: An Alternative to the Standard Model*, Phys. Lett. B **190** (1987) 157.
- [15] C. T. Hill, *Topcolor: Top Quark Condensation In A Gauge Extension Of The Standard Model*, Phys. Lett. B **266** (1991) 419.
- [16] P. Y. Popov, A. V. Povarov and A. D. Smirnov, *Fermionic decays of scalar leptoquarks and scalar gluons in the minimal four color symmetry model*, Mod. Phys. Lett. A **20**, 3003 (2005) [arXiv:hep-ph/0511149].
- [17] I. Dorsner and P. Fileviez Perez, *Unification versus proton decay in $SU(5)$* , Phys. Lett. B **642**, 248 (2006) [hep-ph/0606062].
- [18] P. Fileviez Perez, *Renormalizable adjoint $SU(5)$* , Phys. Lett. B **654**, 189 (2007) [hep-ph/0702287].
- [19] B. A. Dobrescu, K. Kong and R. Mahbubani, *Leptons and photons at the LHC: Cascades through spinless adjoints*, JHEP **0707**, 006 (2007) [arXiv:hep-ph/0703231].
- [20] M. I. Gresham and M. B. Wise, *Color octet scalar production at the LHC*, Phys. Rev. D **76**, 075003 (2007) [arXiv:0706.0909 [hep-ph]].
- [21] I. Dorsner and I. Mocioiu, *Predictions from type II seesaw mechanism in $SU(5)$* , Nucl. Phys. B **796** (2008) 123 [arXiv:0708.3332 [hep-ph]].
- [22] B. A. Dobrescu, K. Kong and R. Mahbubani, *Massive color-octet bosons and pairs of resonances at hadron colliders*, Phys. Lett. B **670**, 119 (2008) [arXiv:0709.2378 [hep-ph]].
- [23] M. Gorbush, T. J. Khoo, D. J. Phalen, A. Pierce and D. Tucker-Smith, *Color-octet scalars at the LHC*, Phys. Rev. D **77** (2008) 095003 [arXiv:0710.3133 [hep-ph]].
- [24] P. Fileviez Perez, H. Minniyaz and G. Rodrigo, *Proton Stability, Dark Matter and Light Color Octet Scalars in Adjoint $SU(5)$ Unification*, Phys. Rev. D **78** (2008) 015013 [arXiv:0803.4156 [hep-ph]].
- [25] P. Fileviez Perez, R. Gavin, T. McElmurry and F. Petriello, *Grand Unification and Light Color-Octet Scalars at the LHC*, Phys. Rev. D **78** (2008) 115017 [arXiv:0809.2106 [hep-ph]].
- [26] T. Plehn and T. M. P. Tait, *Seeking Sgluons*, J. Phys. G **36**, 075001 (2009) [arXiv:0810.3919 [hep-ph]].
- [27] S. Y. Choi, M. Drees, J. Kalinowski, J. M. Kim, E. Poppo and P. M. Zerwas, *Color-Octet Scalars of $N=2$ Supersymmetry at the LHC*, Phys. Lett. B **672**, 246 (2009) [arXiv:0812.3586 [hep-ph]].
- [28] A. Idilbi, C. Kim and T. Mehen, *Factorization and resummation for single color-octet scalar production at the LHC*, arXiv:0903.3668 [hep-ph].
- [29] P. Fileviez Perez and M. B. Wise, *On the Origin of Neutrino Masses*, arXiv:0906.2950 [hep-ph].
- [30] C. P. Burgess, M. Trott and S. Zuberi, *Light Octet Scalars, a Heavy Higgs and Minimal Flavour Violation*, JHEP **0909**, 082 (2009) [arXiv:0907.2696 [hep-ph]].
- [31] J. Shu, T. M. P. Tait and K. Wang, *Explorations of the Top Quark Forward-Backward Asymmetry at the Tevatron*, Phys. Rev. D **81**, 034012 (2010) [arXiv:0911.3237 [hep-ph]].
- [32] A. Arhrib, R. Benbrik and C. -H. Chen, *Forward-backward asymmetry of top quark in diquark models*, Phys. Rev. D **82**, 034034 (2010) [arXiv:0911.4875 [hep-ph]].
- [33] I. Dorsner, S. Fajfer, J. F. Kamenik and N. Kosnik, *Light colored scalars from grand unification and the forward-backward asymmetry in t -bar production*, Phys. Rev. D **81**, 055009 (2010) [arXiv:0912.0972 [hep-ph]].
- [34] I. Dorsner, S. Fajfer, J. F. Kamenik and N. Kosnik, *Light Colored Scalar as Messenger of Up-Quark Flavor Dynamics in Grand Unified Theories*, Phys. Rev. D **82**, 094015 (2010) [arXiv:1007.2604 [hep-ph]].
- [35] K. M. Patel and P. Sharma, *Forward-backward asymmetry in top quark production from light colored scalars in $SO(10)$ model*, JHEP **1104**, 085 (2011) [arXiv:1102.4736 [hep-ph]].
- [36] I. Dorsner, J. Drobnak, S. Fajfer, J. F. Kamenik and N. Kosnik, *Limits on scalar leptoquark interactions and consequences for GUTs*, JHEP **1111**, 002 (2011) [arXiv:1107.5393 [hep-ph]].
- [37] B. Batell, S. Gori and L. -T. Wang, *Exploring the Higgs Portal with 10/fb at the LHC*, JHEP **1206**, 172 (2012)

- [arXiv:1112.5180 [hep-ph]].
- [38] D. C. Stone and P. Uttayarat, *Explaining the $t\bar{t}b\bar{b}$ Forward-Backward Asymmetry from a GUT-Inspired Model*, JHEP **1201**, 096 (2012) [arXiv:1111.2050 [hep-ph]].
 - [39] J. M. Arnold and B. Fornal, *Color octet scalars and high p_T four-jet events at LHC*, Phys. Rev. D **85**, 055020 (2012) [arXiv:1112.0003 [hep-ph]].
 - [40] Y. Bai, J. Fan and J. L. Hewett, *Hiding a Heavy Higgs Boson at the 7 TeV LHC*, JHEP **1208**, 014 (2012) [arXiv:1112.1964 [hep-ph]].
 - [41] B. A. Dobrescu, G. D. Kribs and A. Martin, *Higgs Underproduction at the LHC*, Phys. Rev. D **85**, 074031 (2012) [arXiv:1112.2208 [hep-ph]].
 - [42] W. Altmannshofer, R. Primulando, C. -T. Yu and F. Yu, *New Physics Models of Direct CP Violation in Charm Decays*, JHEP **1204**, 049 (2012) [arXiv:1202.2866 [hep-ph]].
 - [43] K. S. Babu and R. N. Mohapatra, *B-L Violating Nucleon Decay and GUT Scale Baryogenesis in $SO(10)$* , Phys. Rev. D **86**, 035018 (2012) [arXiv:1203.5544 [hep-ph]].
 - [44] S. M. Barr and X. Calmet, *Observable Proton Decay from Planck Scale Physics*, arXiv:1203.5694 [hep-ph].
 - [45] K. Kumar, R. Vega-Morales and F. Yu, *Effects from New Colored States and the Higgs Portal on Gluon Fusion and Higgs Decays*, arXiv:1205.4244 [hep-ph].
 - [46] K. S. Babu and R. N. Mohapatra, *Coupling Unification, GUT-Scale Baryogenesis and Neutron-Antineutron Oscillation in $SO(10)$* , arXiv:1206.5701 [hep-ph].
 - [47] G. D. Kribs and A. Martin, *Enhanced di-Higgs Production through Light Colored Scalars*, Phys. Rev. D **86**, 095023 (2012) [arXiv:1207.4496 [hep-ph]].
 - [48] K. S. Babu and R. N. Mohapatra, *B-L Violating Proton Decay Modes and New Baryogenesis Scenario in $SO(10)$* , arXiv:1207.5771 [hep-ph].
 - [49] S. Calvet, B. Fuks, P. Gris and L. Valery, *Searching for sgluons in multijet events at a center-of-mass energy of 8 TeV*, arXiv:1212.3360 [hep-ph].
 - [50] E. Witten, *Neutrino Masses in the Minimal $O(10)$ Theory*, Phys. Lett. B **91**, 81 (1980).
 - [51] B. Bajc and G. Senjanovic, *Radiative seesaw: A Case for split supersymmetry*, Phys. Lett. B **610**, 80 (2005) [hep-ph/0411193].
 - [52] B. Bajc and G. Senjanovic, *Radiative seesaw and degenerate neutrinos*, Phys. Rev. Lett. **95**, 261804 (2005) [hep-ph/0507169].
 - [53] A. De Rujula, H. Georgi, and S. Glashow, *Flavor Goniometry By Proton Decay*, Phys. Rev. Lett. **45**, 413 (1980).
 - [54] S. M. Barr, *A New Symmetry Breaking Pattern for $SO(10)$ and Proton Decay*, Phys. Lett. B **112**, 219 (1982).
 - [55] D. Chang, R. N. Mohapatra, J. Gipson, R. E. Marshak and M. K. Parida, *Experimental Tests Of New $So(10)$ Grand Unification*, Phys. Rev. D **31**, 1718 (1985).
 - [56] F. Buccella, G. Miele, L. Rosa, P. Santorelli and T. Tuzi, *An Upper Limit For The Proton Lifetime In $So(10)$* , Phys. Lett. B **233**, 178 (1989).
 - [57] N. G. Deshpande, E. Keith and P. B. Pal, *Implications of LEP results for $SO(10)$ grand unification*, Phys. Rev. D **46**, 2261 (1993).
 - [58] F. del Aguila and L. E. Ibanez, *Higgs Bosons in $SO(10)$ and Partial Unification*, Nucl. Phys. B **177**, 60 (1981).
 - [59] R. N. Mohapatra and G. Senjanovic, *Higgs Boson Effects in Grand Unified Theories*, Phys. Rev. D **27**, 1601 (1983).
 - [60] K. I. Aoki, Z. Hioki, M. Konuma, R. Kawabe and T. Muta, *Electroweak Theory. Framework of On-Shell Renormalization and Study of Higher Order Effects*, Prog. Theor. Phys. Suppl. **73**, 1 (1982).
 - [61] S. Weinberg, *Effective Gauge Theories*, Phys. Lett. B **91**, 51 (1980).
 - [62] D. R. T. Jones, *Two Loop Diagrams in Yang-Mills Theory*, Nucl. Phys. B **75**, 531 (1974).
 - [63] W. E. Caswell, *Asymptotic Behavior of Nonabelian Gauge Theories to Two Loop Order*, Phys. Rev. Lett. **33**, 244 (1974).
 - [64] D. R. T. Jones, *The Two Loop beta Function for a $G(1) \times G(2)$ Gauge Theory*, Phys. Rev. D **25**, 581 (1982).
 - [65] M. E. Machacek and M. T. Vaughn, *Two Loop Renormalization Group Equations in a General Quantum Field Theory. 1. Wave Function Renormalization*, Nucl. Phys. B **222**, 83 (1983).
 - [66] L. N. Mihaila, J. Salomon and M. Steinhauser, *Renormalization constants and beta functions for the gauge couplings of the Standard Model to three-loop order*, Phys. Rev. D **86**, 096008 (2012) [arXiv:1208.3357 [hep-ph]].
 - [67] W. Martens, L. Mihaila, J. Salomon and M. Steinhauser, *Minimal Supersymmetric $SU(5)$ and Gauge Coupling Unification at Three Loops*, Phys. Rev. D **82**, 095013 (2010) [arXiv:1008.3070 [hep-ph]].
 - [68] J. Beringer et al. [Particle Data Group Collaboration], *Review of Particle Physics (RPP)*, Phys. Rev. D **86**, 010001 (2012).
 - [69] L. J. Hall, *Grand Unification Of Effective Gauge Theories*, Nucl. Phys. B **178**, 75 (1981).
 - [70] P. Nath and P. Fileviez Perez, *Proton stability in grand unified theories, in strings and in branes*, Phys. Rept. **441**, 191 (2007) [hep-ph/0601023].
 - [71] P. Fileviez Perez, *Fermion mixings versus $d = 6$ proton decay*, Phys. Lett. B **595**, 476 (2004) [hep-ph/0403286].
 - [72] I. Dorsner and P. Fileviez Perez, *How long could we live?*, Phys. Lett. B **625**, 88 (2005) [hep-ph/0410198].
 - [73] H. Nishino et al. [Super-Kamiokande Collaboration], *Search for Nucleon Decay into Charged Anti-lepton plus Meson in Super-Kamiokande I and II*, Phys. Rev. D **85**, 112001 (2012) [arXiv:1203.4030 [hep-ex]].
 - [74] K. Abe, T. Abe, H. Aihara, Y. Fukuda, Y. Hayato, K. Huang, A. K. Ichikawa and M. Ikeda et al., *Letter of Intent: The Hyper-Kamiokande Experiment — Detector Design and Physics Potential —*, arXiv:1109.3262 [hep-ex].
 - [75] X. Calmet, S. D. H. Hsu and D. Reeb, *Grand unification and enhanced quantum gravitational effects*, Phys. Rev. Lett. **101**, 171802 (2008) [arXiv:0805.0145 [hep-ph]].
 - [76] J. Chakraborty and A. Raychaudhuri, *A Note on dimension-5 operators in GUTs and their impact*, Phys. Lett. B **673**, 57 (2009) [arXiv:0812.2783 [hep-ph]].
 - [77] S. Bertolini, L. Di Luzio and M. Malinsky, *Structure and prospects of the simplest $SO(10)$ GUTs*, arXiv:1210.3789 [hep-ph].
 - [78] R. S. Chivukula and H. Georgi, *Composite Technicolor Standard Model*, Phys. Lett. B **188**, 99 (1987).
 - [79] L. J. Hall and L. Randall, *Weak scale effective supersymmetry*, Phys. Rev. Lett. **65**, 2939 (1990).
 - [80] G. D'Ambrosio, G. F. Giudice, G. Isidori and A. Strumia, *Minimal flavor violation: An Effective field theory approach*, Nucl. Phys. B **645**, 155 (2002) [hep-ph/0207036].
 - [81] B. Bajc, A. Melfo, G. Senjanovic and F. Vissani, *Yukawa sector in nonsupersymmetric renormalizable $SO(10)$* ,

- Phys. Rev. D **73**, 055001 (2006) [hep-ph/0510139].
- [82] K. S. Babu and R. N. Mohapatra, *Predictive neutrino spectrum in minimal $SO(10)$ grand unification*, Phys. Rev. Lett. **70**, 2845 (1993) [hep-ph/9209215].
 - [83] A. S. Joshipura and K. M. Patel, *Fermion Masses in $SO(10)$ Models*, Phys. Rev. D **83**, 095002 (2011) [arXiv:1102.5148 [hep-ph]].
 - [84] G. Lazarides, *$So(10)$ And The Invisible Axion*, Phys. Rev. D **25**, 2425 (1982).
 - [85] R. Holman, G. Lazarides and Q. Shafi, *Axions And The Dark Matter Of The Universe*, Phys. Rev. D **27**, 995 (1983).
 - [86] R. N. Mohapatra and G. Senjanovic, *The Superlight Axion And Neutrino Masses*, Z. Phys. C **17**, 53 (1983).
 - [87] J. E. Kim and G. Carosi, *Axions and the Strong CP Problem*, Rev. Mod. Phys. **82**, 557 (2010) [arXiv:0807.3125 [hep-ph]].
 - [88] M. Nemevsek, G. Senjanovic and Y. Zhang, *Warm Dark Matter in Low Scale Left-Right Theory*, JCAP **1207**, 006 (2012) [arXiv:1205.0844 [hep-ph]].
 - [89] J. Erler, *Tests of the Electroweak Standard Model*, arXiv:1209.3324 [hep-ph].
 - [90] G. Aad *et al.* [ATLAS Collaboration], *ATLAS search for new phenomena in dijet mass and angular distributions using pp collisions at $\sqrt{s} = 7$ TeV*, JHEP **1301**, 029 (2013) [arXiv:1210.1718 [hep-ex]].
 - [91] S. Chatrchyan *et al.* [CMS Collaboration], *Search for narrow resonances and quantum black holes in inclusive and b -tagged dijet mass spectra from pp collisions at $\sqrt{s} = 7$ TeV*, JHEP **1301**, 013 (2013) [arXiv:1210.2387 [hep-ex]].
 - [92] G. Aad *et al.* [ATLAS Collaboration], *Search for pair-produced massive colored scalars in four-jet final states with the ATLAS detector in proton-proton collisions at $\sqrt{s} = 7$ TeV*, Eur.Phys.J. **C73**, 2263 (2013) [arXiv:1210.4826 [hep-ex]].
 - [93] S. Chatrchyan *et al.* [CMS Collaboration], *Search for pair-produced dijet resonances in four-jet final states in pp collisions at $\sqrt{s} = 7$ TeV*, (2013) [arXiv:1302.0531 [hep-ex]].
 - [94] S. Bertolini, L. Di Luzio and M. Malinsky, work in progress.